Chapter 10
Functions of G-Protein-Coupled Receptors and Ion Channels and the Downstream Cytoplasmic Signals in the Regulation of Toxicity of Environmental Toxicants or Stresses

Abstract It is an assumption that environmental toxicants or stresses will first activate or suppress certain G-protein-coupled receptors (GPCRs) and/or ion channels on the surface of targeted cells and then activate a subset of downstream cytoplasmic signaling cascades. Based on this assumption, we here first introduced and discussed the involvement of GPCRs (epidermal DCAR-1, intestinal FSHR-1, neuropeptide receptors, and neuronal SRH-220) and ion channels (cyclic nucleotide-gated ion channel, voltage-gated calcium ion channel, potassium ion channel, and chloride intracellular channel) in the regulation of toxicity of environmental toxicants or stresses and the underlying mechanisms. Moreover, we discussed the potential activation of cytoplasmic signaling cascade, containing ARR-1/arrestin, G-proteins, PLC-DAG-PKD signaling, and Ca^{2+} signaling, upon the exposure to environmental toxicants or stresses and the corresponding important functions.

Keywords G-protein-coupled receptors (GPCRs) · Ion channel · Cytoplasmic signaling cascade · Environmental exposure · *Caenorhabditis elegans*

10.1 Introduction

In nematodes, various environmental toxicants/stresses can induce the alterations in different aspects on animals [1–17]. Upon the exposure to environmental toxicants/stresses, it is assumed that certain G-protein-coupled receptors (GPCRs) or ion channels would be activated or suppressed. After that, a certain downstream cytoplasmic signaling cascade will be affected, and the functions of certain transcriptional factors and their targets will be further altered. If this assumption is correct and the toxic effects of toxicants or stresses can reach the targeted organs (especially the primary targeted organs), both the GPCRs and the ion channels play crucial roles in the induction of toxicity in nematodes exposed to environmental toxicants or stresses.

In this chapter, we first introduced the identified GPCRs involved in the regulation of toxicity of environmental toxicants or stresses and the underlying mechanisms for their important functions. Again, we introduced and discussed the

D. Wang, *Molecular Toxicology in Caenorhabditis elegans*,
https://doi.org/10.1007/978-981-13-3633-1_10

involvement of several types of ion channels in the regulation of toxicity of environmental toxicants or stresses. Moreover, we focused on ARR-1/arrestin, G-proteins, PLC-DAG-PKD signaling, and Ca^{2+} signaling to discuss the important functions of cytoplasmic signaling cascade in transducing environmental stimuli and mediating the toxicity induction in nematodes exposed to environmental toxicants or stresses.

10.2 GPCRs

In Chaps. 5, 6, and 9, we have discussed the functions of some important GPCRs, such as insulin receptors, Wnt receptors, and neurotransmitter receptors, in regulating the toxicity of environmental toxicants or stresses and the underlying mechanisms. We here further introduced and discussed the involvement of other GPCRs in the regulation of toxicity of environmental toxicants and stresses and the underlying mechanisms.

10.2.1 Epidermal DCAR-1

Infection with environmental pathogens (bacterial pathogens and fungal pathogens) will cause toxicity at various aspects on both human beings and animals, including the nematodes [18–24]. With the fungus *Drechmeria coniospora* as an example, RNAi knockdown was performed on 1150 GPCR-encoding genes to identify the GPCRs required for the control of innate immunity against the fungal infection [25, 26]. Based on the expression of an antimicrobial peptide (AMP) reporter gene (*nlp-29p::gfp*), three clones, targeting *dcar-1* (*dcar-1(RNAi)*), *frpr-11* (*frpr-11(RNAi)*), and *srv-21 (srv-21(RNAi)*), were found to be able to decrease the expression of the reporter gene (Fig. 10.1) [26]. The *sta-1* (*sta-1*(*RNAi*)) was used as a control, since it does not affect expression of the gene-encoding GFP. Meanwhile, it was observed that, unlike *frpr-11(RNAi)* or *srv-21(RNAi)*, *dcar-1(RNAi)* did not affect the expression of *nlp-29p::gfp* in nematodes expressing a constitutively active form of the Gα protein GPA-12 (Fig. 10.1) [26], suggesting that the DCAR-1 may act upstream or in parallel to GPA-12. *dcar-1(RNAi)* also could not abrogate the *nlp-29* induction by osmotic stress (Fig. 10.1) [26].

In nematodes, DCAR-1 acted in the epidermis to regulate the expression of AMP-encoding genes and the defense against fungal infection [26]. Meanwhile, it was found that mutation of *dcar-1* had a profound effect on the induction of six *nlp* genes in nematodes infected with *D. coniospora* (Fig. 10.1) [26]. Among them, the activation of DCAR-1 was due to the endogenous ligands of NLP-28 and NLP-29, and loss-of-function mutation of *dcar-1* (in a *dpy-10;dcar-1* mutant) reduced the elevated expression of *nlp-29* [26].

In the epidermis, the dihydrocaffeic acid (DHCA) was identified as an exogenous ligand that activates the innate immune response via DCAR-1. The addition of

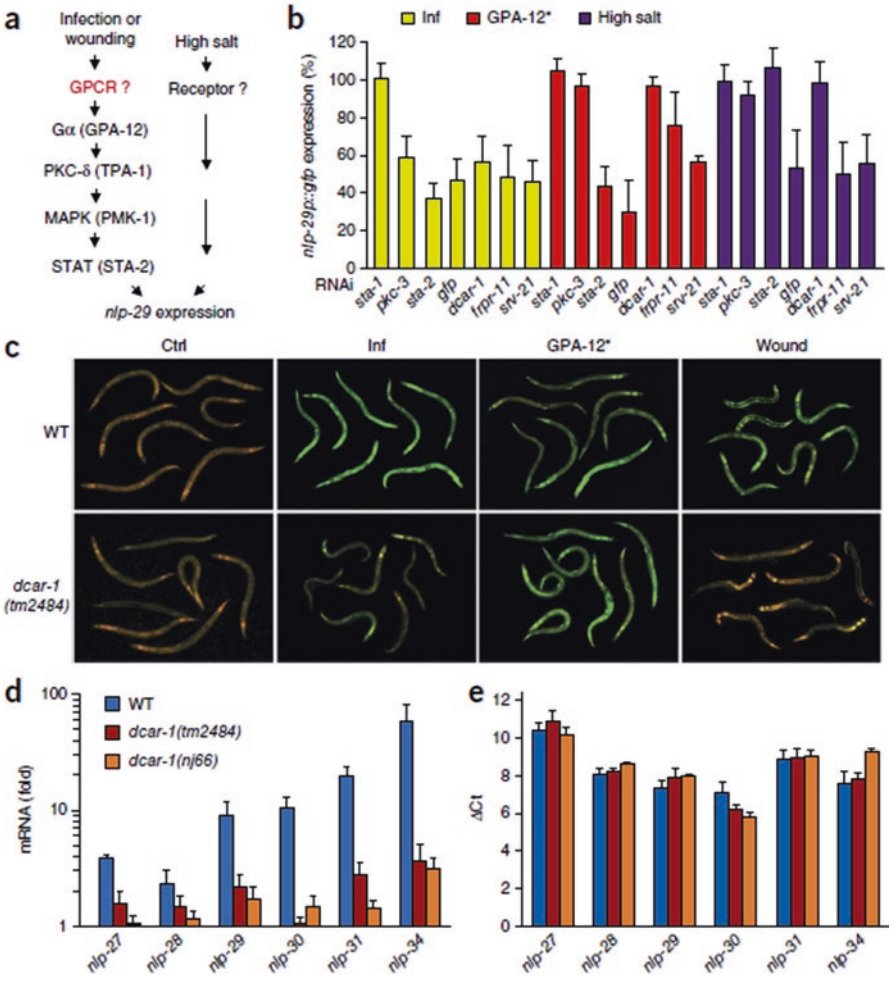

Fig. 10.1 The GPCR DCAR-1 controls the expression of AMP-encoding genes [26]. (**a**) Pathways that lead to the expression of *nlp-29*. (**b**) Expression of *nlp-29p::gfp* by worms carrying the integrated array *frIs7* (which contains the reporter transgenes *nlp-29::gfp* and *col-12::DsRed*) and treated by RNAi directed against control or candidate genes (horizontal axis) and infected with *D. coniospora* (Inf) or expressing the constitutively active GPA-12* in the epidermis (GPA-12*) or exposed to a high salt medium (high salt); results are normalized GFP fluorescence presented relative to results obtained with the negative control *sta-1(RNAi)*, set as 100%. (**c**) Fluorescent images of wild-type (WT) and *dcar-1(tm2484)* worms carrying *frIs7* and assessed without further treatment (control (Ctrl)) or after infection by *D. coniospora* (Inf) or expressing GPA-12* in the epidermis (GPA-12*) or assessed after wounding (wound). Constitutive expression of DsRed in the epidermis is unaffected by these treatments. Original magnification, ×600 (images obtained with a filter set to visualize green and red fluorescence). (**d**) Quantitative RT-PCR analysis of the expression of genes in the *nlp-29* cluster (horizontal axis) in wild-type, *dcar-1(tm2484)*, and *dcar-1(nj66)* worms after infection with *D. coniospora*; results are presented relative to those of uninfected worms. (**e**) Abundance of mRNA of genes in the *nlp-29* cluster in the wild-type, *dcar-1(tm2484)*, and *dcar-1(nj66)* strains, presented as the change in cycling threshold (ΔCt) calculated as the cycling threshold for each *nlp* gene minus that for the gene-encoding actin (*act-1*). Data are from experiments with at least six biological replicates (**b**; with at least 50 worms per condition; mean and s.d.) or are representative of over ten experiments (**c**) or are from three independent experiments (**d**, **e**; average and s.d.)

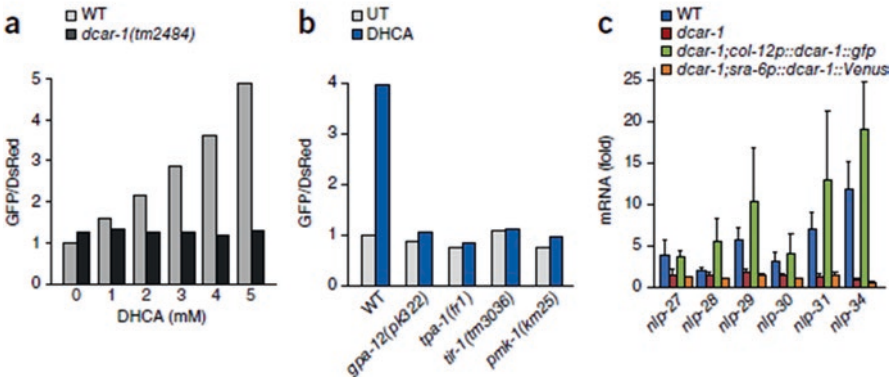

Fig. 10.2 DHCA mimics the effect of infection on the expression of AMP-encoding genes [26]. (**a**, **b**) Fluorescence ratio of green (GFP) to red (DsRed) of wild-type and *dcar-1(tm2484)* worms ($n \geq 50$ per condition) carrying *frIs7* and treated with increasing concentrations of DHCA; results are normalized to those of wild-type worms. (**b**) Fluorescence ratio (as in **a**, **b**) of wild-type and various mutant strains ($n > 50$ per condition) carrying *frIs7* and left untreated (UT) or treated with 5 mM DHCA (key). (**c**) Quantitative RT-PCR analysis of the expression of genes in the *nlp-29* cluster in wild-type, *dcar-1(tm2484)*, *dcar-1;col-12p·dcar-1::gfp*, and *dcar-1;sra-6p·dcar-1::Venus* mutant worms after exposure for 2 h to 5 mM DHCA; results are presented relative to those of uninfected control worms. Data representative of four experiments (**a**, **b**) or are from two experiments (**c**; average and s.d. of three biological replicates)

DHCA to wild-type nematodes could trigger the expression of the *nlp-29p::gfp* reporter gene in a dose-dependent manner (Fig. 10.2) [26]. This increase was blocked in *dcar-1* mutant nematodes or in nematodes in which various elements of regulatory network controlling the *nlp-29* expression were mutant (*gap-12*, *tpa-1*, *tir-1*, or *pmk-1*) (Fig. 10.2) [26]. In addition, treatment with DHCA also triggered an increase in the *nlp-29* expression, and this increase was dependent on *dcar-1* and *pmk-1* (Fig. 10.2) [26]. More importantly, the expression of *dcar-1* in the epidermis, not in the neurons, was sufficient to restore the induction of *nlp* genes by DHCA (Fig. 10.2) [26].

Four molecules (DHPA (3-(2 4-dihydroxyphenyl)propionic acid), DHCA, DPPA, and HPLA) that are structurally related to DHCA were identified as in vivo ligands for DCAR-1 and could trigger the *nlp-29p::gfp* expression in a dose-dependent manner (Fig. 10.3) [26]. Nevertheless, DHCA beyond the concentration of 80 mM was toxic, and DPPA, DHPA, and HPLA were toxic at concentrations above 10 mM [26]. Moreover, based on the analysis of high-performance liquid chromatography, the HPLA was present at a low level in control nematodes and could be increased ~3.5-fold by fungal infection (Fig. 10.3) [26].

Additionally, since the HPLA amount was elevated in extracts of pellets of *dpy-10* mutant nematodes, HPLA could be generated as a consequence of alterations in cuticle development [26]. The *nlp-29p::gfp* expression increase induced by HPLA was also dependent on DCAR-1 and various elements of downstream signal transduction cascade (*gpa-12*, *tpa-1*, *tir-1*, and *pmk-1*) (Fig. 10.3) [26], suggesting that

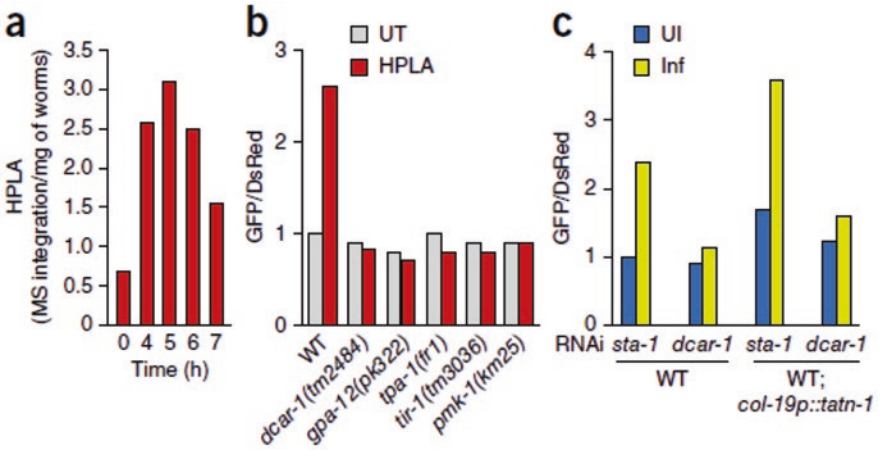

Fig. 10.3 Endogenous HPLA increases upon infection with *D. coniospora* and triggers the expression of *nlp-29* AMP-encoding genes via a DCAR-1–PMK-1 signaling pathway [26]. (**a**) Abundance of HPLA in wild-type worms at various times (horizontal axis) after infection with *D. coniospora*, presented as integration of high-performance liquid chromatography–mass spectrometry (MS) peaks, normalized to the worm pellet dry weight. (**b**) Fluorescence ratio of wild-type and mutant worms (horizontal axis) carrying *frIs7*, left untreated or treated with 5 mM HPLA (key). (**c**) Fluorescence ratio of wild-type worms (left) or wild-type that additionally carry an epidermally expressed construct *col-19p::tatn-1* (right), left uninfected or infected with *D. coniospora* and treated by RNAi with control or *dcar-1*-targeting clones (horizontal axis). Data are representative of two experiments (**a**) or experiments with at least three (**b**) or two (**c**) biological replicates of at least 50 worms per condition

HPLA can act through the DCAR-1 to regulate the epidermal innate immune response in nematodes.

10.2.2 Intestinal FSHR-1

Of the 14 candidate LRR receptors, GPCR FSHR-1 was identified as a putative innate immune receptor. After infection with Gram-negative or Gram-positive bacterial pathogens, the *fshr-1(ok778)* mutant nematodes exhibited more sensitive than wild-type nematodes to the killing (Fig. 10.4) [27]. Meanwhile, the *fshr-1(ok778)* mutant nematodes do not have a reduced lifespan on *E. coli* OP50, suggesting the susceptibility of *fshr-1(ok778)* mutant nematodes to pathogen infection is not due to the nonspecific sickness [27].

More importantly, FSHR-1 regulated transcription of a set of putative antimicrobial genes that can be induced by pathogen infection. Three of five PMK-1-dependent genes (*F56D6.2*, *C17H12.8*, and *F49F1.6*) induced by PA14 were decreased in *fshr-1(ok778)* mutant nematodes (Fig. 10.5) [27]. Besides this, the expression inductions of at least *F01D5.5* and *C32H11.12* upon PA14 exposure

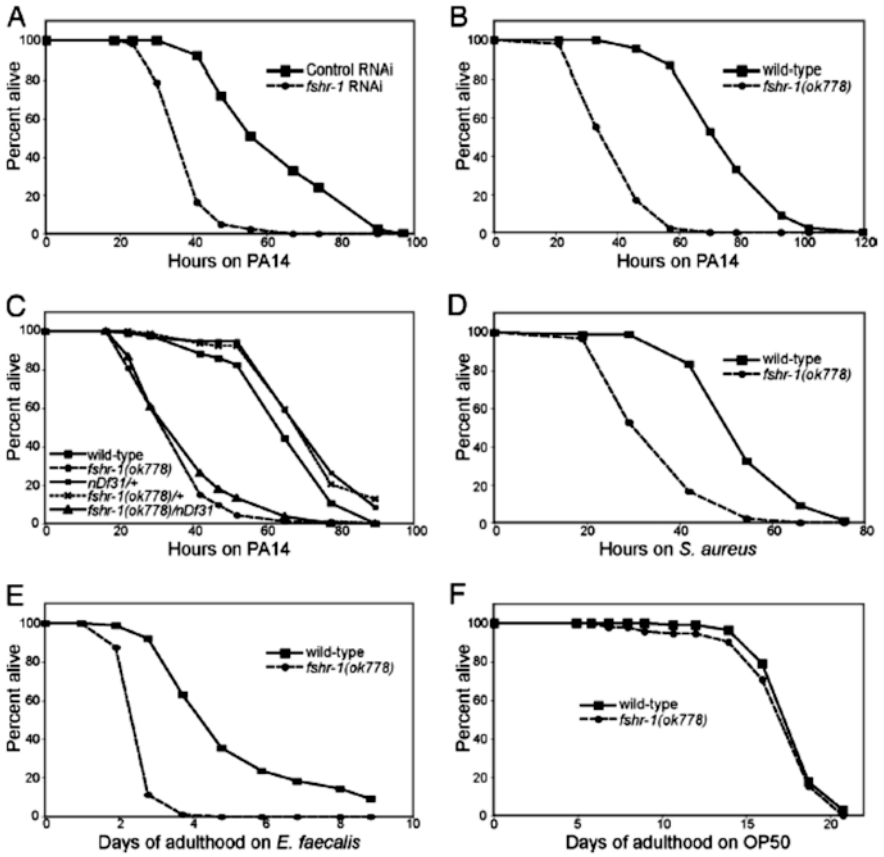

Fig. 10.4 FSHR-1 is required for innate immunity [27]. (**a**, **b**) *fshr-1* (RNAi) or *fshr-1(ok778)* mutant worms are sensitive to killing by pathogenic *P. aeruginosa* PA14 relative to wild-type control worms. (**c**) *fshr-1(ok778)/nDf31* heterozygotes are just as sensitive to PA14 as *fshr-1(ok778)* homozygotes. (**d**–**f**) *fshr-1(ok778)* mutants are sensitive to killing by pathogenic *S. aureus* and *E. faecalis* but not to *E. coli* OP50

were reduced in *fshr-1(ok778)* mutant nematodes (Fig. 10.5) [27], suggesting that their expression was independent of PMK-1 but dependent on the FSHR-1 in response to pathogen infection in nematodes.

Tissue-specific activity analysis demonstrated that FSHR-1 functioned in the intestine, the major site of pathogen exposure, to regulate the innate immunity [27]. During the control of innate immunity to pathogen infection, FSHR-1 acted in parallel to both the insulin (*daf-2*) and the p38 MAPK (*tir-1*, *nsy-1*, and *pmk-1*) pathways. It was found that *daf-2(e1368ts); fshr-1(ok778)* double mutants had an immunity phenotype that was intermediate between either of the single mutants (Fig. 10.6) [27]. Additionally, *pmk-1(km25);fshr-1(ok778)* double mutants were even more sensitive than either single mutants, and mutation of *tir-1* or *nsy-1* significantly enhanced the *fshr-1(ok778)* null phenotype (Fig. 10.6) [27].

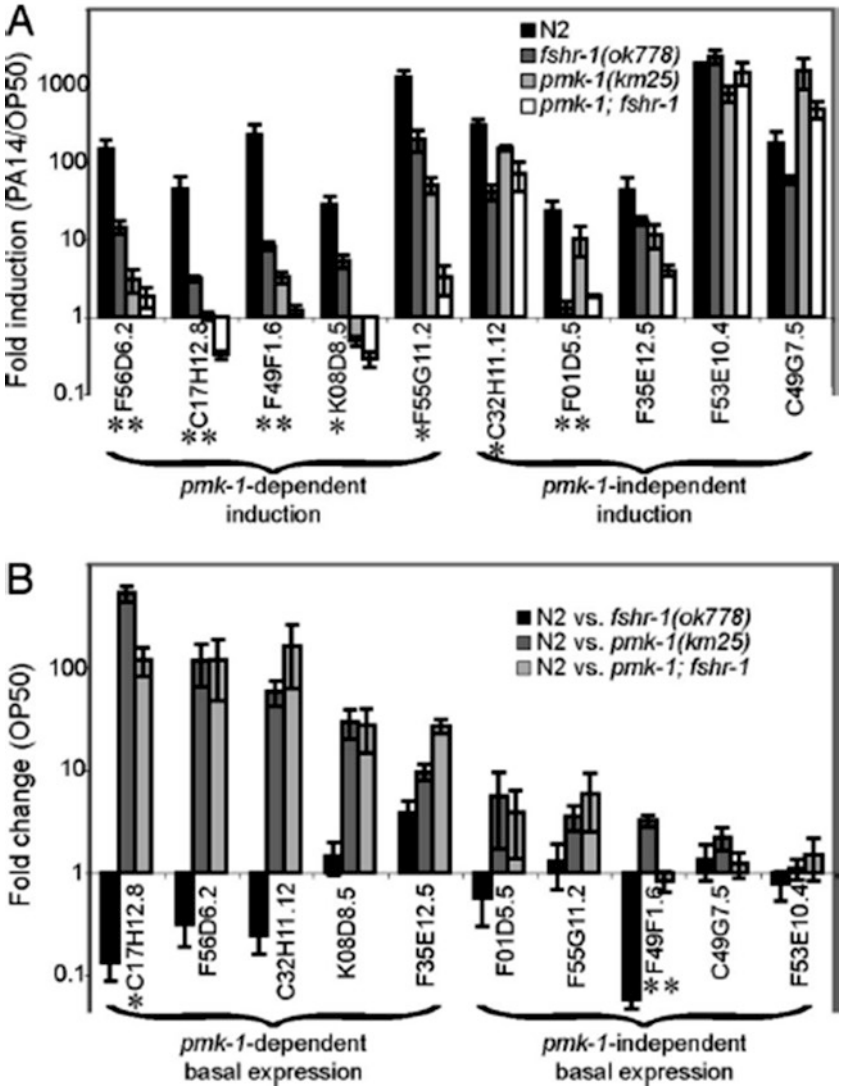

Fig. 10.5 FSHR-1 regulates PA14 response genes [27]. (**a**, **b**) qRT-PCR was used to analyze the relative transcription of PA14 response genes in wild-type and mutant worms fed OP50 or PA14. Error bars represent SEM for three independent biologic replicates. (**a**) Fold induction was calculated as the ratio of normalized expression on PA14 divided by expression on OP50. *Genes with greater than fivefold reduction in their induction in *fshr-1(ok778)* mutant worms relative to wild-type worms with $P < 0.01$. **Genes with greater than tenfold reduction in their induction in *fshr-1(ok778)* mutants relative to wild-type with $P < 0.01$. (**b**) Fold change in basal expression was calculated as the ratio of wild-type expression to mutant expression in worms fed OP50. *Genes with greater than fivefold lower basal expression in wild-type worms relative to *fshr-1(ok778)* mutants. **Genes with greater than tenfold lower basal expression in wild-type worms relative to *fshr-1(ok778)* mutants

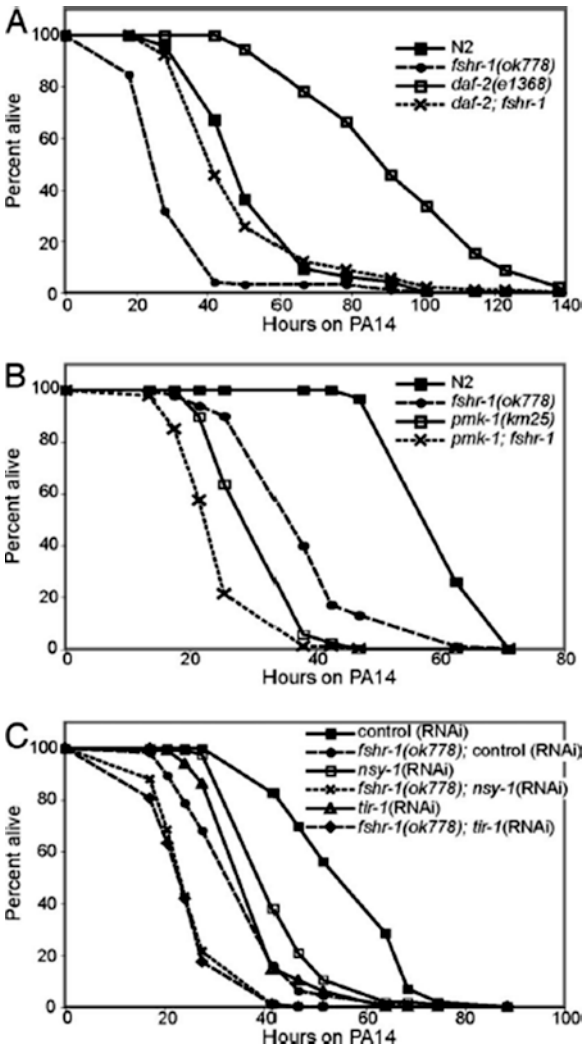

Fig. 10.6 FSHR-1 acts in parallel to DAF-2 and the p38 MAPK pathway [27]. (**a**) *daf-2* and *fshr-1* single and double mutants were raised at 15 °C and then shifted to the restrictive temperature of 25 °C 4 h before exposure to PA14. (**b**, **c**) Loss of components of the p38 MAPK pathway, either by genetic mutation (*pmk-1*) or RNAi (*tir-1* and *nsy-1*), enhances the pathogen sensitivity of *fshr-1(ok778)* null mutants. Experiments with *pmk-1* and *fshr-1* single and double mutants were repeated five times, and in all cases the double mutants were significantly more sensitive than either single mutant

10.2.3 Neuropeptide Receptors

10.2.3.1 NPR-1

Based on the mutant screen, it was found that the *npr-1(ad609)* mutant nematodes showed the enhanced susceptibility to *P. aeruginosa*-mediated killing (Fig. 10.7) [28]. Under the normal conditions, no difference in survival was seen between *npr-1(ad609)* mutant and wild-type nematodes [28], suggesting that the *npr-1* mutation affects the innate immune response to pathogenic bacteria without altering the basic lifespan. Additionally, although the lawn avoidance is part of *C. elegans* defense

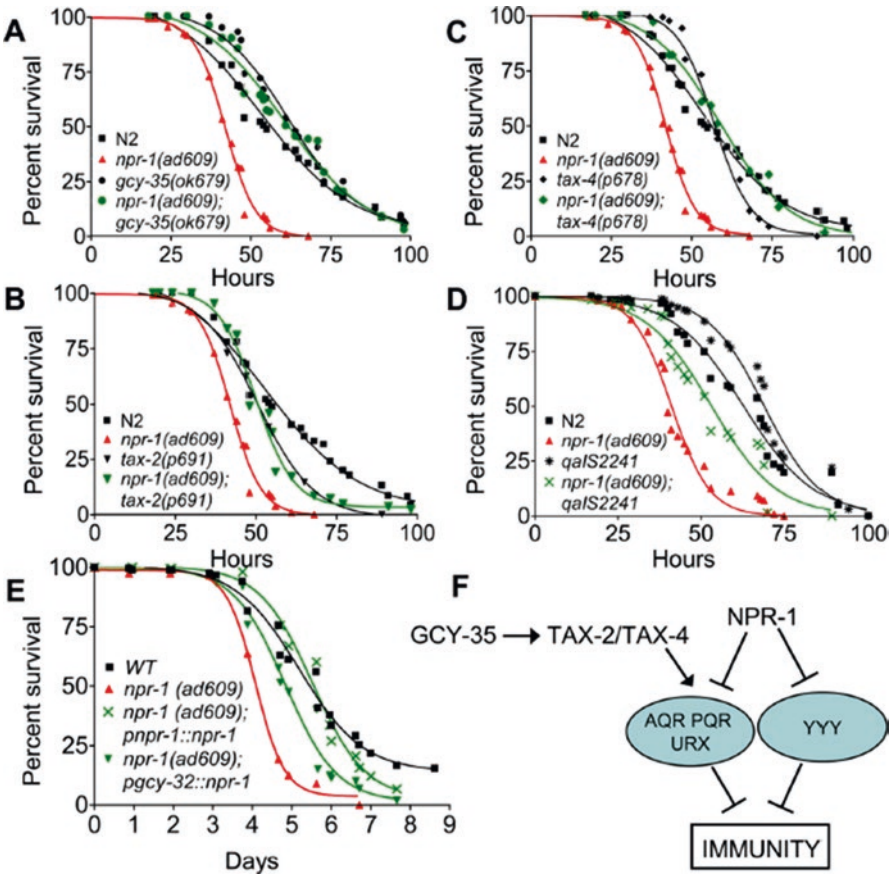

Fig. 10.7 The NPR-1 neural circuit regulates innate immunity [28]. (**a**) Wild-type N2, *npr-1(ad609)* ($P = 0.0001$), *gcy-35(ok769)* ($P = 0.0125$), and *gcy-35(ok769);npr-1(ad609)* ($P = 0.0639$) were exposed to *P. aeruginosa*. (**b**) Wild-type N2, *npr-1(ad609)* ($P = 0.0001$), *tax-4(p678)* ($P = 0.1673$), and *tax-4(p678);npr-1(ad609)* ($P = 0.3611$) were exposed to *P. aeruginosa*. (**c**) Wildtype N2, *npr-1(ad609)* ($P = 0.0001$), *tax-2(p691)* ($P = 0.0930$), and *tax-2(p691);npr-1(ad609)* ($P = 0.0031$) were exposed to *P. aeruginosa*. (**d**) Wild-type N2; *npr-1(ad609)* ($P = 0.0001$); *qaIS2241* ($P = 0.0042$); a strain which lacks AQR, PQR, and URX neurons; and *npr-1(ad609);qaIS2241* ($P = 0.0001$) were exposed to *P. aeruginosa.* The graphs represent combined results of at least three independent experiments, $N \geq 40$ adult nematodes per strain. (**e**) Wild-type N2, *npr-1(ad609)* ($P = 0.0001$), p*gcy-32::npr-1; npr-1(ad609)* ($P = 0.0001$), and p*npr-1::npr-1;npr-1(ad609)* ($P = 0.1939$) were exposed to *P. aeruginosa.* The graphs represent combined results of at least two independent experiments, $N \geq 100$ adult nematodes per strain. Killing assays were performed at 17 °C, as low temperatures are known to increase the resolution of killing assays involving *P. aeruginosa.* (**f**) Model of the neural control of innate immunity in *C. elegans*: NPR-1 inhibits the activity of AQR, PQR, URX and additional neuron(s) designated YYY that suppress innate immunity, while GCY-35, TAX-2, and TAX-4 are required for the activation of AQR, PQR, and URX neurons

response to *P. aeruginosa,* it did not account for the difference between wild-type and *npr-1(ad609)* animals [28]. The susceptibility of nematodes deficient in NPR-1 to *P. aeruginosa* was largely due to the decreased pathogen avoidance and the decreased innate immune responses.

In nematodes, the enhanced susceptibility of *npr-1(ad609)* to *P. aeruginosa* could be rescued by mutations in *gcy-35* soluble guanylate cyclase (Fig. 10.7) [28]. Moreover, *npr-1*- and *gcy-35*-expressing sensory neurons (AQR, PQR, and URX) could actively suppress the innate immune responses of non-neuronal tissues to pathogen infection, since the nematodes lacking AQR, PQR, and URX neurons exhibited an increased survival on *P. aeruginosa* (Fig. 10.7) [28]. In addition, killing the AQR, PQR, and URX neurons also partially rescued the enhanced susceptibility of *npr-1(ad609)* to *P. aeruginosa* (Fig. 10.7) [28]. Expression of *npr-1* in the AQR, PQR, and URX neurons could rescue the enhanced susceptibility of *npr-1(ad609)* to *P. aeruginosa* (Fig. 10.7) [28], suggesting the requirement of NPR-1 activity in sensory neurons for the control of innate immunity.

A full-genome microarray analysis was performed to identify the downstream targets for NPR-1 in regulating innate immunity in nematodes subjecting to pathogen infection. It was found that mutation in *npr-1* caused the alteration of genes that are markers of innate immune responses, including those regulated by a conserved PMK-1/p38 MAPK signaling pathway (Fig. 10.8) [28]. These genes were similarly misregulated in nematodes deficient in NPR-1 or PMK-1 function [28]. Additionally, the *npr-1(ad609)* nematodes showed lower levels of active PMK-1 than wild-type nematodes (Fig. 10.8) [28]. Nevertheless, RNAi knockdown of *pmk-1* in *npr-1(ad609)* mutant nematodes resulted in an increased susceptibility to pathogen infection [28], suggesting that NPR-1 regulates both PMK-1-dependent and independent innate immune responses in nematodes.

10.2.3.2 NPR-4

Using assay system of preference choice on bacterial foods, OP50 and pathogen PA14, it was observed that the ADL sensory neurons were required for the control of preference choice [29]. In nematodes, some neuropeptides encoded by *flp-4*, *flp-21*, *nlp-7*, *nlp-8*, and *nlp-10* are expressed in ADL sensory neurons, and ADL-specific RNAi knockdown of *flp-4* or mutation of *nlp-10* significantly decreased choice index compared with wild-type N2 [29].

The receptor for neuropeptide FLP-4 is NPR-4. Loss-of-function mutation of *npr-4* significantly decreased the choice index compared with wild-type N2 (Fig. 10.9) [29]. In nematodes, the sensory inputs can be released from ADL sensory neurons to AIA, AIB, AVA, AVB, or AVD interneurons (Fig. 10.9) [29]. Expression of NPR-4 in the AVA or AIA interneurons did not recover the deficit in preference choice in *npr-4(tm1782)* mutants (Fig. 10.9) [29]. In contrast, expression of NPR-4 in AIB interneurons could obviously rescue the deficit in preference choice in *npr-4(tm1782)* mutants (Fig. 10.9) [29], suggesting that the FLP-4 released

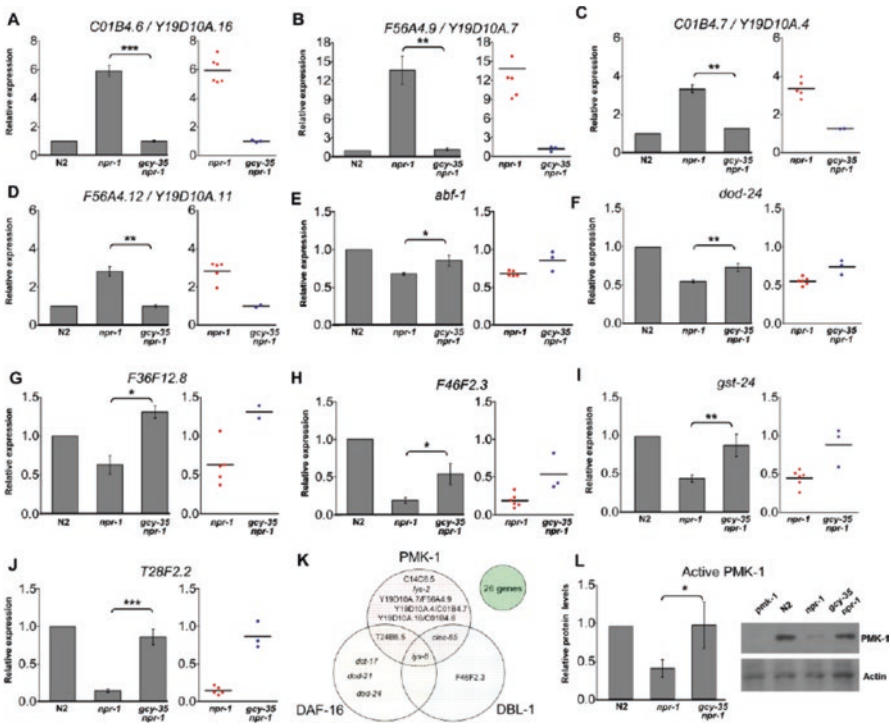

Fig. 10.8 The NPR-1 neural circuit regulates expression of innate immune genes [28]. (**a**–**j**) Quantitative reverse transcription–PCR analysis of *C01B4.6/Y19D10A.16*, *F56A4.9/Y19D10A.7*, *C01B4.7/Y19D10A.4*, *F56A4.12/Y19D10A.11*, *abf-1*, *dod-24*, *F36F12.8*, *F46F2.3*, *gst-24*, and *T28F2.2* expression in *npr-1(ad609)* and *gcy-35(ok769);npr-1(ad609)* nematodes relative to wild-type nematodes exposed to *P. aeruginosa*. Data were analyzed by normalization to actin *(act-1,-3,-4)* and relative quantification using the comparative cycle threshold method. Student's exact *t*-test indicates differences among the groups are significantly different; bar graphs correspond to mean ± SEM. Point graphs correspond to gene quantification in independent isolations of *npr-1(ad609)*($N = 6$) and *gcy-35(ok769);npr-1(ad609)* ($N = 3$). (K) The Venn diagram lists the genes identified by microarray analysis to be regulated by both NPR-1 and one or more known innate immune pathways in *C. elegans*. Genes that lie within two or three circles are regulated by multiple innate immune pathways in addition to NPR-1. Twenty-six genes have not been previously connected to any of the innate immune pathways and are depicted in the solitary circle. (L) Immunological detection of active PMK-1. Active PMK-1 was detected in wild-type N2, *npr-1(ad609)*, and *gcy-35(ok769);npr-1(ad609)*. Animals were grown at 20 °C until 1-day-old adult and whole worm lysates were used to detect active PMK-1 by Western blotting using an antihuman p38 antibody. Actin was detected using a polyclonal antibody

from ADL sensory neurons regulates the preference choice through its receptor of NPR-4 in AIB interneurons in nematodes.

To identify candidate targeted genes for *npr-4* in regulating preference choice, the expression patterns of genes expressed in AIB interneurons were examined. Among 24 genes expressed in AIB interneurons, it was found that mutation of *npr-4* caused the significant increase in expression levels of *ptp-3* and *ced-10* and the

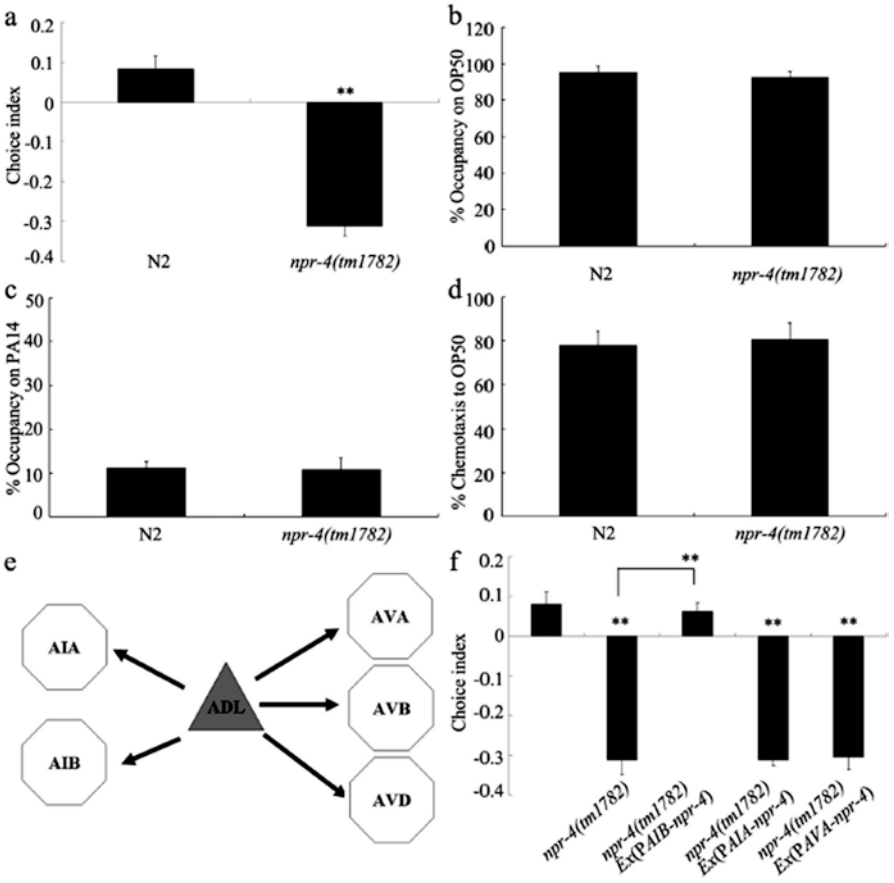

Fig. 10.9 NPR-4 regulated the preference choice in nematodes [29]. (**a**) Mutation of *npr-4* gene altered preference choice. (**b**–**d**) Mutation of *npr-4* gene did not influence leaving behavior from bacterial lawns and chemotaxis to OP50. (**e**) Schematic diagram for putative neural networks associated with ADL sensory neurons, extracted from the complete circuit. Sensory neurons are shown as triangles and interneurons as hexagons. Arrows indicate chemical synapses. (**f**) Expression of NPR-4 in AIB interneurons rescued the deficit in preference choice in *npr-4* mutants. Bars represent means ± S.E.M. $^{**}P < 0.01$ vs N2 (if not specifically indicated)

significant decrease in expression levels of *glr-2*, *tax-6*, *cdc-42*, and *set-2* (Fig. 10.10) [29]. Using the available mutants for candidate targeted genes of *npr-4* to investigate their possible function in regulating preference choice, it was observed that only mutation of *set-2* caused the significant decrease in choice index compared with wild-type N2 (Fig. 10.10) [29]. In nematodes, *set-2* encodes a histone H3 at lysine 4 (H3K4) methyltransferase. Moreover, preference choice phenotype of double mutant of *set-2(ok952);npr-4(tm1782)* was similar to that of single mutant of *set-2(ok952)* or *npr-4(tm1782)* (Fig. 10.10) [29], suggesting that SET-4 and NPR-4 function in the same pathway to regulate preference choice.

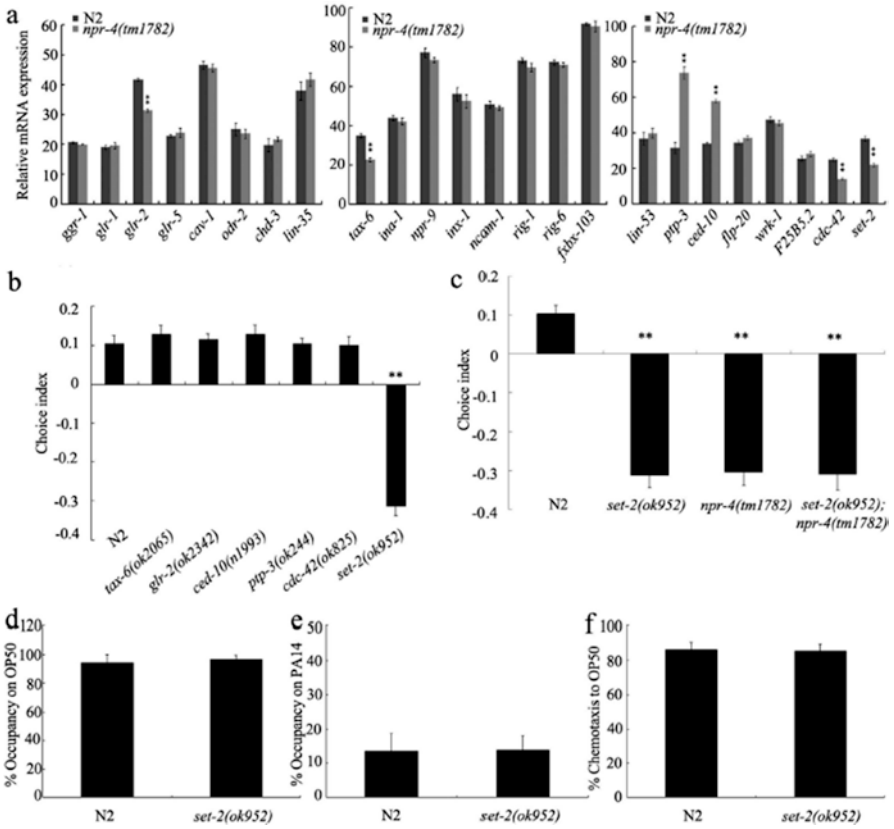

Fig. 10.10 Identification of downstream target for NPR-4 in regulating preference choice in nematodes [29]. (**a**) Mutation of *npr-4* gene altered expression patterns of some genes expressed in AIB interneurons. (**b**) Mutation of *set-2* gene induced the deficit in preference choice. (**c**) Genetic interaction of *npr-4* with *set-2* in regulating preference choice. (**d**–**f**) Leaving behavior from bacterial lawns and chemotaxis to OP50 in *set-2* mutants. Bars represent means ± S.E.M. $^{**}P < 0.01$ vs N2

10.2.3.3 NPR-9

npr-9 encodes a homolog of the gastrin-releasing peptide receptor (GRPR) and is expressed in AIB interneurons. After infection with *P. aeruginosa* PA14, the *npr-9(tm1652)* mutant nematodes showed a resistance to the PA14 infection, a decreased PA14 colonization, and an increased expression of some immunity-related genes (Fig. 10.11) [30]. In contrast, the nematodes overexpressing NPR-9 exhibited an increased susceptibility to infection, an increased PA14 colonization, and a reduced expression of some immunity-related genes [30]. Additionally, the expression of GRPR, the human homolog of NPR-9, could largely mimic the NPR-9 function in regulating the innate immunity against the pathogen infection in nematodes [30].

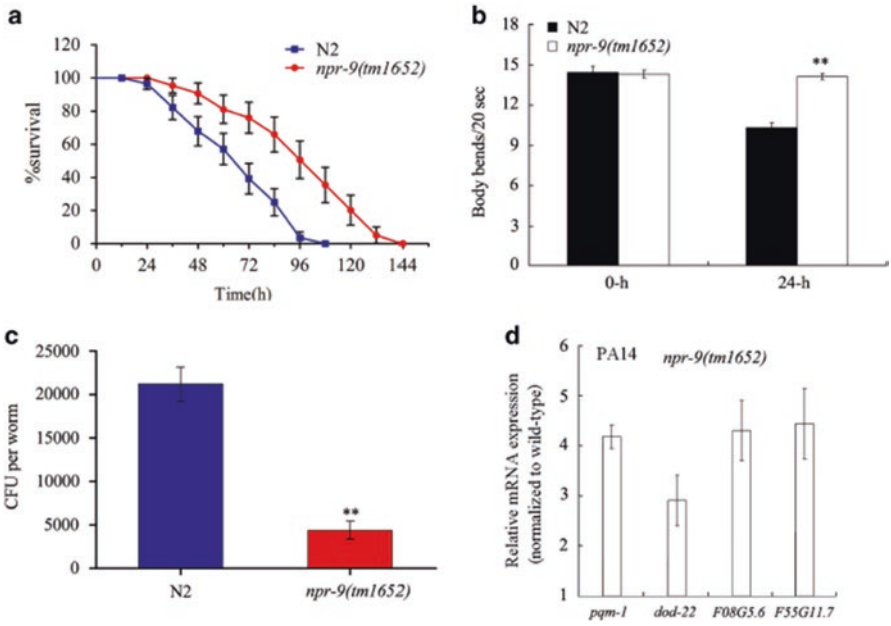

Fig. 10.11 *npr-9* mutants were resistant to *P. aeruginosa* infection [30]. (**a**) Comparison of survival plots between wild-type N2 and *npr-9* mutants exposed to *P. aeruginosa* PA14. A statistical comparison of the survival plots indicates that survival of the mutant animals was significantly different from that of wild-type N2 animals ($P < 0.0001$). (**b**) Comparison of body bend between wild-type N2 and *npr-9* mutants exposed to *P. aeruginosa* PA14 for 24 h. Bars represent mean ± s.d. $^{**}P < 0.01$ vs N2. (**c**) Comparison of CFU between wild-type N2 and *npr-9* mutants exposed to *P. aeruginosa* PA14. Bars represent the mean ± s.d. $^{**}P < 0.01$ vs N2. (**d**) Quantitative real-time PCR analysis of expression patterns for immunity-related genes in *npr-9* mutants exposed to *P. aeruginosa* PA14. Normalized expression is presented relative to wild-type expression; bars represent the mean ± s.d.

ChR2-mediated AIB interneuron activation could strengthen the innate immune response and decrease the PA14 colonization [30]. In nematodes, synaptic transmission can be potentiated by expression of the active protein kinase C homolog *(pkc-1(gf))* [31, 32]. More importantly, it was observed that the overexpression of NPR-9 suppressed the innate immune response and increased PA14 colonization in nematodes with the activation of AIB interneurons mediated by ChR2 or by expressing *pkc-1(gf)* in AIB interneurons (Fig. 10.12) [30]. Therefore, it is hypothesized that NPR-9 regulates the innate immune response to pathogen infection by antagonizing the activity of AIB interneurons.

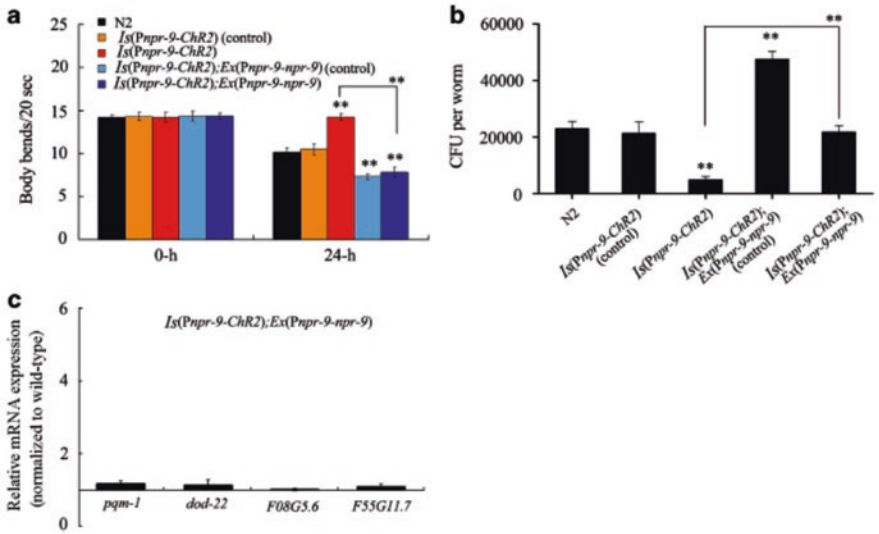

Fig. 10.12 NPR-9 antagonized the function of AIB interneurons to regulate innate immunity [30]. (**a**) Effects of *npr-9* overexpression on body bend of nematodes with ChR2-mediated activation in AIB interneurons exposed to *P. aeruginosa* PA14. (**b**) Effects of *npr-9* overexpression on CFU in nematodes with ChR2-mediated AIB interneuron activation exposed to *P. aeruginosa* PA14. (**c**) Effects of *npr-9* overexpression on expression patterns for immunity-related genes in nematodes with ChR2-mediated activation of AIB interneurons exposed to *P. aeruginosa* PA14. Normalized expression is presented relative to wild-type expression. Bars represent the mean ± s.d. $^{**}P < 0.01$ vs N2 if not specially indicated. CFU, colony-forming unit

10.2.3.4 NPR-12

NLP-29 is a neuropeptide-like protein expressed in the epidermis. The NLP-29 expression can be induced by infection with pathogens, such as *Drechmeria coniospora* (36-h exposure) [33]. Infection of *D. coniospora* caused significant PVD dendrite degeneration, and mutation of *nlp-29* was able to completely block the infection-induced PVD dendrite degeneration (Fig. 10.13) [33].

The neuronal GPCR NPR-12 was further identified as the receptor of NLP-29 in nematodes [33]. Similarly, mutation of *npr-12* also completely blocked the infection-induced PVD dendrite degeneration (Fig. 10.13) [33]. Compared to aging-associated degeneration, the rate of degeneration induced by infections at day 1 was relatively low (Fig. 10.13) [33], which might be due to protective mechanisms in young animals. Additionally, in infected nematodes, FLP dendrites displayed significantly higher degeneration rates, and mutation of *nlp-29* or *npr-12* also blocked this FLP degeneration caused by infection (Fig. 10.13) [33]. Nevertheless, pathogen infection did not induce obvious degeneration of PLM dendrites/sensory processes (Fig. 10.13) [33]. However, ectopic expression of *npr-12* in PLM neurons was sufficient to cause infection-dependent degeneration, and *nlp-29* mutation could suppress this effect (Fig. 10.13) [33]. Moreover, mutations of *atg-4.1* were able to

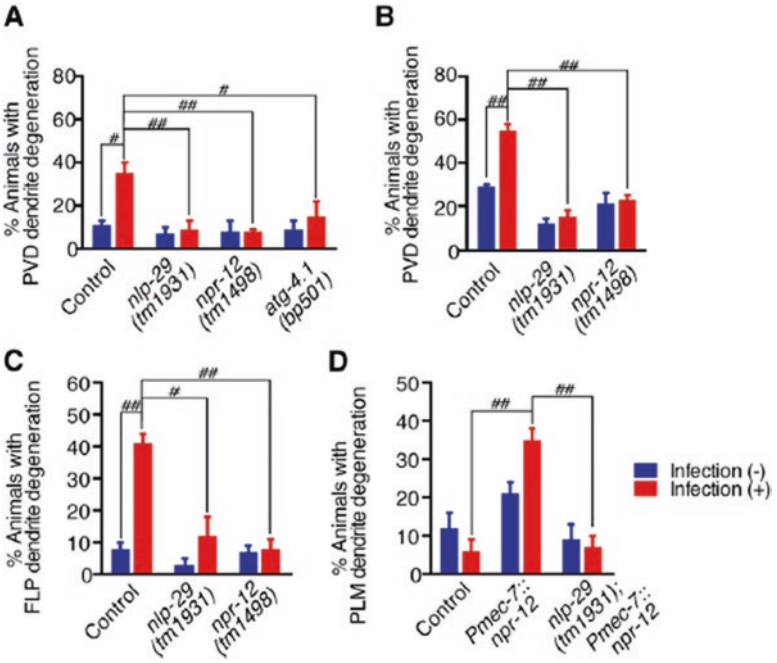

Fig. 10.13 Fungal infection induces dendrite degeneration via NLP-29 and NPR-12 [33]. Animals were either treated with *Drechmeria coniospora* or vehicle solution (NaCl 50 mM) and were quantified for dendrite degeneration after 36-h incubation in the pathogen or vehicle. The mean differences between each strain under different treatment conditions were analyzed by one-way ANOVA, followed by Fisher's LSD post hoc test. (**a**) Effects of infection on PVD dendrite degeneration; animals were treated on day 1. (**b**) Effects of infection on PVD dendrite degeneration; animals were treated on day 3. (**c**) Effects of infection on FLP dendrite degeneration; animals were treated on day 1. (**d**) Effects of infection on degeneration of PLM dendrite/sensory processes; animals were treated on day 1; ectopic expression of *npr-12* in PLM neurons was driven by the *mec-7* promoter (P*mec-7::npr-12*). #$p < 0.05$; ##$p < 0.001$. Data are represented as mean ± SEM

completely block the infection-induced PVD dendrite degeneration (Fig. 10.13) [33], implying that the autophagic machinery may be involved downstream of NPR-12 to transduce the degeneration signals in nematodes.

10.2.4 Neuronal SRH-220

Some genes encoding GPCRs such as SRE-1, SRI-51, SRH-132, and SRH-220 are expressed in the ADL sensory neurons, and, among them, loss-of-function mutation of *srh-220* resulted in an enhanced choice index compared with wild-type N2 (Fig. 10.14) [29], suggesting that the ADL can regulate the preference choice by inhibiting the function of GPCR SRH-220.

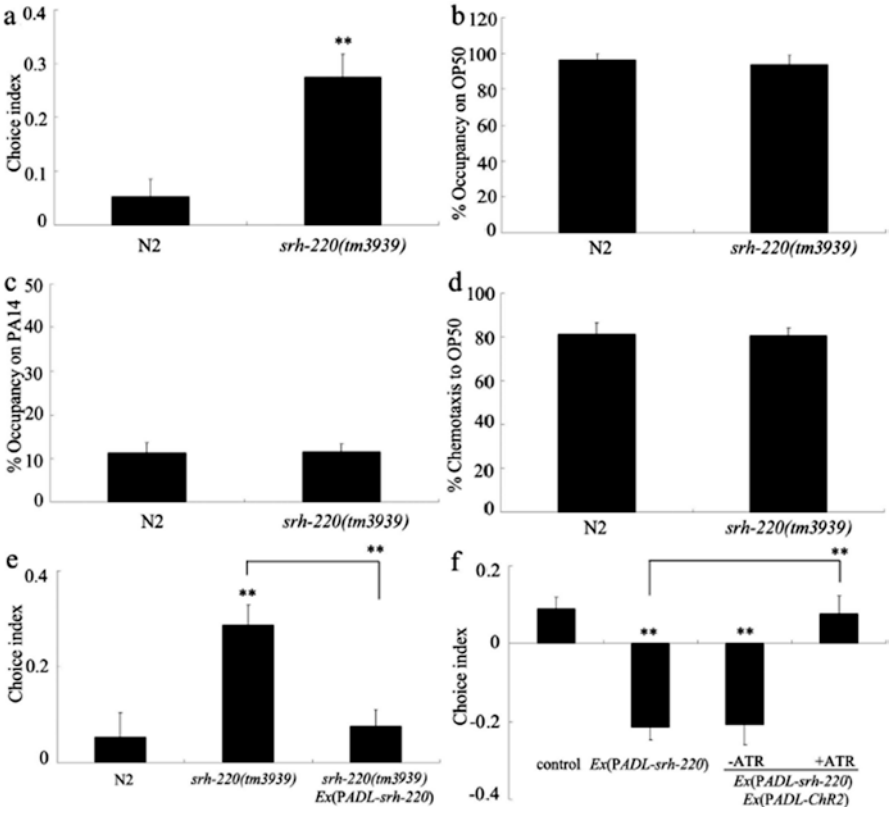

Fig. 10.14 Roles of SRH-220/GPCR in ADL sensory neurons in the control of preference choice in nematodes [29]. (**a**) Effects of *srh-220* mutation on preference choice. (**b**–**d**) Leaving behavior from bacterial lawns and chemotaxis to OP50 in *srh-220* mutants. (**e**) Rescue assay of preference choice phenotype in *srh-220* mutants. (**f**) Optogenetically activating ADL sensory neurons suppressed the function of SRH-220 in regulating preference choice. Optogenetical activation was performed under the *lite-1* mutation background. Control, *lite-1(ce314)*. Bars represent means ± S.E.M. $^{**}P < 0.01$ vs N2 (if not specifically indicated)

In nematodes, *unc-31* encodes a DAG-binding protein that plays a key role in dense core vesicle (DCV) release, and ADL RNAi knockdown of *unc-31* significantly decreased the choice index [29]. *gsa-1* encodes a Gαs that enhances exocytosis from DCVs, and *pde-4* encodes a phosphodiesterase to alter cAMP levels. Similarly, ADL RNAi knockdown of *gsa-1* or *pde-4* significantly decreased the choice index [29]. These observations imply that the signaling from ADL sensory neurons may be primarily peptidergic with respect to the control of preference choice. In other words, the ADL sensory neurons might regulate preference choice through peptidergic signals, such as FLP-4 and NLP-10 [29].

Moreover, it was found that the function of FLP-4 or NLP-10 in regulating the preference choice was regulated by SRH-220. The preference choice phenotype in

double mutant of *flp-4(RNAi);srh-220(tm3783)* was similar to that in *flp-4(RNAi)* nematodes, and the preference choice phenotype in double mutant of *nlp-10(tm6232);srh-220(tm3783)* was similar to that in *nlp-10(tm6232)* mutant nematodes [29]. Therefore, *flp-4* or *nlp-10* mutation may suppress the preference choice phenotype in *srh-220* mutant nematodes.

10.3 Ion Channels

10.3.1 Cyclic Nucleotide-Gated Ion Channels

10.3.1.1 TAX-2 and TAX-4

In nematodes, the enhanced susceptibility of *npr-1(ad609)* mutant nematodes to *P. aeruginosa* was rescued by mutations in *tax-2* or *tax-4*, encoding a cyclic GMP-gated ion channel [28], suggesting the involvement of these two ion channels in regulating the function of NPR-1 in controlling the innate immunity to pathogen infection in nematodes.

10.3.1.2 CNG-3

CNG-3 shows high homology with CNG channels of higher animals, as well as the TAX-4 [34]. CNG-3 is restricted in five sensory neurons of amphid, including AFD neurons [34]. Although the *cng-3* null mutant nematodes displayed a normal chemotaxis to volatile odorants, the *cng-3* mutant nematodes exhibited an impaired thermal tolerance (Fig. 10.15) [34]. Moreover, the *tax-4; cng-3* double mutants showed a similar phenotype to *tax-4* mutants (Fig. 10.15) [34], suggesting that TAX-4 may act downstream of CNG-3 to regulate the thermal stress in nematodes.

10.3.2 Voltage-Gated Calcium Ion Channel UNC-2

UNC-2 is an ortholog of voltage-gated calcium ion channel protein. Under the normal conditions, UNC-2 functions to antagonize the transforming growth factor TGF-β pathway to influence the movement rate [35]. This UNC-2/TGF-β pathway was required for the accumulation of normal serotonin levels, because the decreased serotonergic staining in the ADF neurons of *unc-2* mutant nematodes could be suppressed by *daf-4* and *unc-43(gf)* mutations [35]. This UNC-2/TGF-β pathway was further required for the thermal stress-induced tryptophan hydroxylase (TPH-1) expression in serotonergic chemosensory ADF neurons, but not the NSM neurons (Fig. 10.16) [35]. Moreover, this thermal stress-induced *tph-1::GFP* expression could be restored to normal level in the ADF neurons in *unc-2* mutant nematodes by

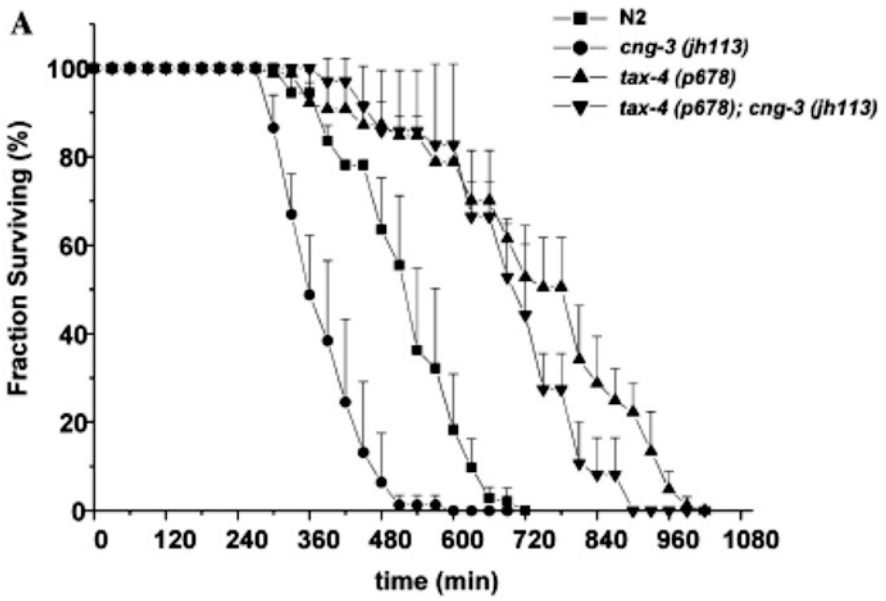

B

Worm strain	Mean survival (± SEM)
N2	475 (± 22) min
cng-3 (jh113)	357 (± 16)
tax-4 (p678)	707 (± 10)
tax-4 (p678) ; cng-3 (jh113)	666 (± 34)

Fig. 10.15 Thermotolerance assay of *cng-3* [34]. (**a**) Fraction of survived worms was scored during thermal stress of three plates containing 30 animals of each strain. Each data point represents the mean fraction of live worms over three plates at each time point. (**b**) The survival times of each strain are shown in mean ± SEM: wild type, 475 ± 22 min ($n = 73$); *cng-3*, 357 ± 16 min ($n = 77$); *tax-4*, 707 ± 10 min ($n = 80$); and *tax-4;cng-3* double mutants, 666 ± 34 min ($n = 65$). The *cng-3* mutants were significantly more sensitive than wild type ($P < 0.0001$)

mutations in *daf-4* gene in TGF-β pathway or by *unc-43(gf)* mutation [35]. Besides this, it was found that transgenic expression of migraine-associated Ca^{2+} channel, CACNA1A, in *unc-2* mutant nematodes could also functionally substitute for UNC-2 in stress-activated regulation of *tph-1* expression [35].

10.3.3 Potassium Ion Channel KVS-1

KVS-1 is a potassium ion channel protein. In nematodes, the oxidation of KVS-1 during the aging could cause the sensory function loss, and protection of this KVS-1 channel from the oxidation could preserve the neuronal function [36]. Moreover, it

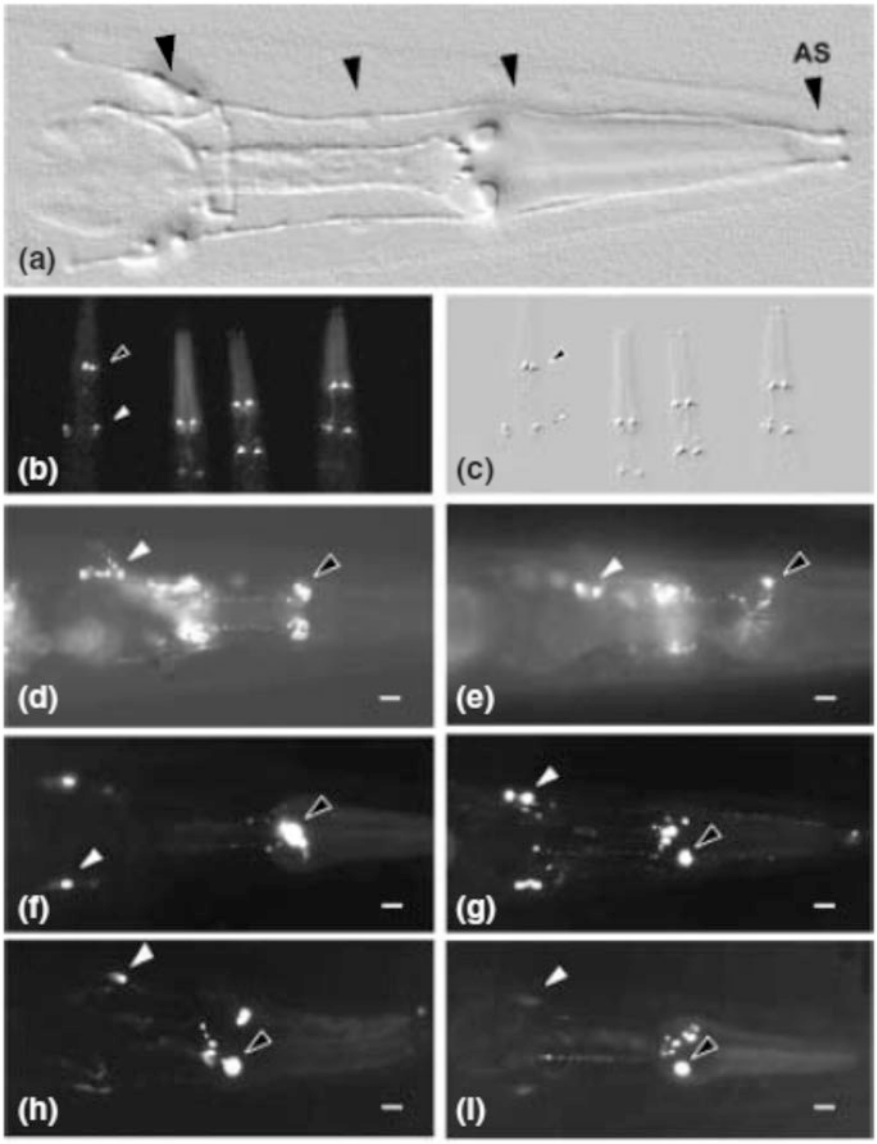

Fig. 10.16 UNC-2 is required for stress-mediated regulation of *tph-1* expression in ADF [35]. (**a**) The *tph-1* expression in the ADF neuron is emphasized in an embossed fluorescence stereomicroscope image of a WT animal grown at 25 °C. The identity of the cell indicated by the outlined arrowhead as the ADF neuron is confirmed by both the position of the cell body near the distal end of the NSM axonal process and the extension of its dendritic process (black arrowheads) to the amphid sensillum (AS). (**b, c**) Decreased *tph-1::GFP* expression observed in the ADF neurons of fed *unc-2* adult animals grown at 25 °C is increased by *unc-43(gf)* and *daf-4(m592)*. Animals arranged for fluorescence (**b**) stereomicroscopy were embossed (**c**) as described above to emphasize the differences observed between strains in the intensity of the ADF neurons; left to right: WT,

was found that the chemotaxis, a function controlled by KVS-1, was impaired in nematodes exposed to oxidizing agents, but only moderately affected in nematodes with an oxidation-resistant KVS-1 mutant (C113S) (Fig. 10.17) [36]. The endogenous ROS could modify the native KVS-1 channels, and the native KVS-1 currents could be modified by endogenous ROS or by oxidizing agents [36]. In nematodes, the KVS-1 conducted the A-type current in the ASER sensory neurons.

10.3.4 Chloride Intracellular Channel EXL-1

Under the thermal stress conditions, EXL-1, not the EXC-4, responded specifically to the heat stress and translocated from the cytoplasm to the nucleus in intestinal cells in a timely ordered manner from posterior to anterior region and body wall muscle cells (Fig. 10.18) [37]. EXL-1 bears a nonclassical nuclear localization signal (NLS). Meanwhile, it was found that the *exl-1* loss-of-function mutant nematodes were susceptible to heat stress than wild-type nematodes [37].

10.4 ARR-1/Arrestin

ARR-1 is the sole GPCR adaptor protein arrestin-1 in the GPCR signaling. The arrestins can block the G-protein-mediated signaling and itself function as signal transducers [38]. In nematodes, ARR-1 is expressed exclusively and functions within the nervous system to regulate the innate immunity against the pathogen infection (Fig. 10.19) [38]. ARR-1 regulated both the pathogen resistance and the lifespan extension by targeting different pathways [38]. ARR-1 was required for the GPCR signaling in ADF, AFD, ASH, ASI, AQR, PQR, and URX neurons to regulate the innate immune response to pathogen infection (Fig. 10.19) [38]. As indicated by the expressional alteration in *abu* genes, the ER UPR induction in *arr-1(ok401)* mutant nematodes was independent of OCTR-1 in ASH and ASI sensor neurons [38], suggesting that ARR-1 regulates the innate immune response to pathogen infection by activating the ER UPR response in nematodes.

Fig. 10.16 (continued) *unc-2*, *unc-2;unc-43(gf)*, and *unc-2;daf-4(m592)*. (**d, e**) Monoaminergic differentiation of the ADF neurons is normal in *unc-2*. Expression of the monoamine transporter gene reporter *cat-1::GFP* is similar in WT (d) and *unc-2* (**e**). (**f–i**) *tph-1::GFP* expression in the ADF neurons is regulated by temperature and starvation. Expression of the *tph-1* transgene in ADF is weaker than in NSM at 15 °C (**f**) but nearly equal at 25 °C (**g**) in fed WT animals. Fed *unc-2* animals have low levels of *tph-1* transgene expression in the ADF as in (**f**), at both 15 and 25 °C, but frequently exhibit unilateral (**h**) or absent (**i**) ADF expression when developing to the adult under relative starvation conditions at 25 °C. The location of the ADF and NSM neurons is indicated by white and black arrowheads, respectively. Scale bars, 10 μm

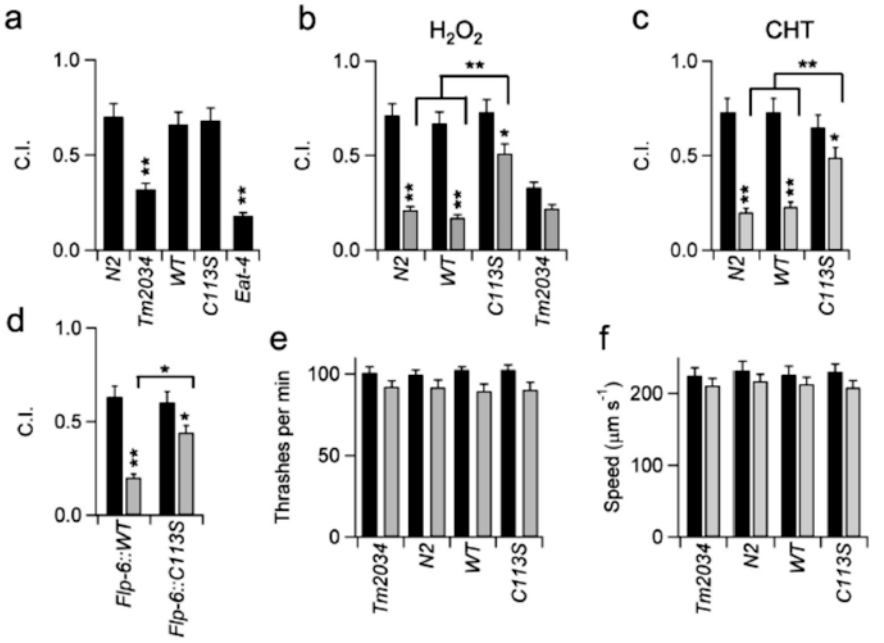

Fig. 10.17 Protected chemosensory function in C113S worms [36]. (**a**) Chemotaxis to biotin in *N2* (parental control strain), *tm2034* (*kvs-1* null), *wild type-KVS-1* (WT), and *C113S-KVS-1* (C113S), L4 worms. The chemotaxis-defective *eat-4(ky5)*, which harbors a mutation in a vesicular glutamate transporter necessary for glutamatergic neurotransmission in *C. elegans*, was employed as "sensory-defective" positive control. $n = 4$ experiments. (**b**) Chemotaxis to biotin in control conditions (black) and in worms exposed to hydrogen peroxide (light gray). Young adult worms were soaked in M9 buffer containing 1 mM H_2O_2 (for 20 min) or M9 buffer (control), allowed to recover for 30 min, transferred to a test plate, and tested for chemotaxis. $n = 5$ experiments for *N2*, *wild type-KVS-1*, and *C113S-KVS-1* and $n = 3$ experiments for *kvs-1* KO. (**c**) As in B for worms exposed to 0.5 mM CHT for 40 min. $n = 5$ experiments. (**d**) As in B for *Pflp-6::wild type-KVS-1* and *Pflp-6::C113S-KVS-1* worms. $n = 4$ experiments. (**e**) Forward movement phenotype in the indicated genotypes in control (black) and after exposure to 1 mM H_2O_2 (light gray). $n \geq 11$ animals/bar. (**f**) Mean average speeds in the indicated genotypes in control (black) and after exposure to 1 mM H_2O_2 (light gray). $n \geq 10$ animals/bar. Data are presented as mean ± standard error of the mean (s.e.m). Statistically significant differences are indicated with * ($0.01 < P < 0.05$) and ** ($P < 0.01$)

Fig. 10.18 (continued) (D1–D3) EXL-1::GFP translocates into the nucleus in body wall muscle cells (arrows) under heat shock at 35 °C for 2 h. Inset shows enlarged image of the nucleus. (E1–E3) DAPI staining in L4 animals shows that EXL-1::GFP signal overlaps with DNA staining inside the nucleus. (F1-F3) EXL-1::GFP does not translocate into the nucleus under 200 mM paraquat treatment for 4 h. Images are taken at L4 stage. 1, GFP fluorescence image; 2, Nomarski image (E2: DAPI staining); 3, merged image

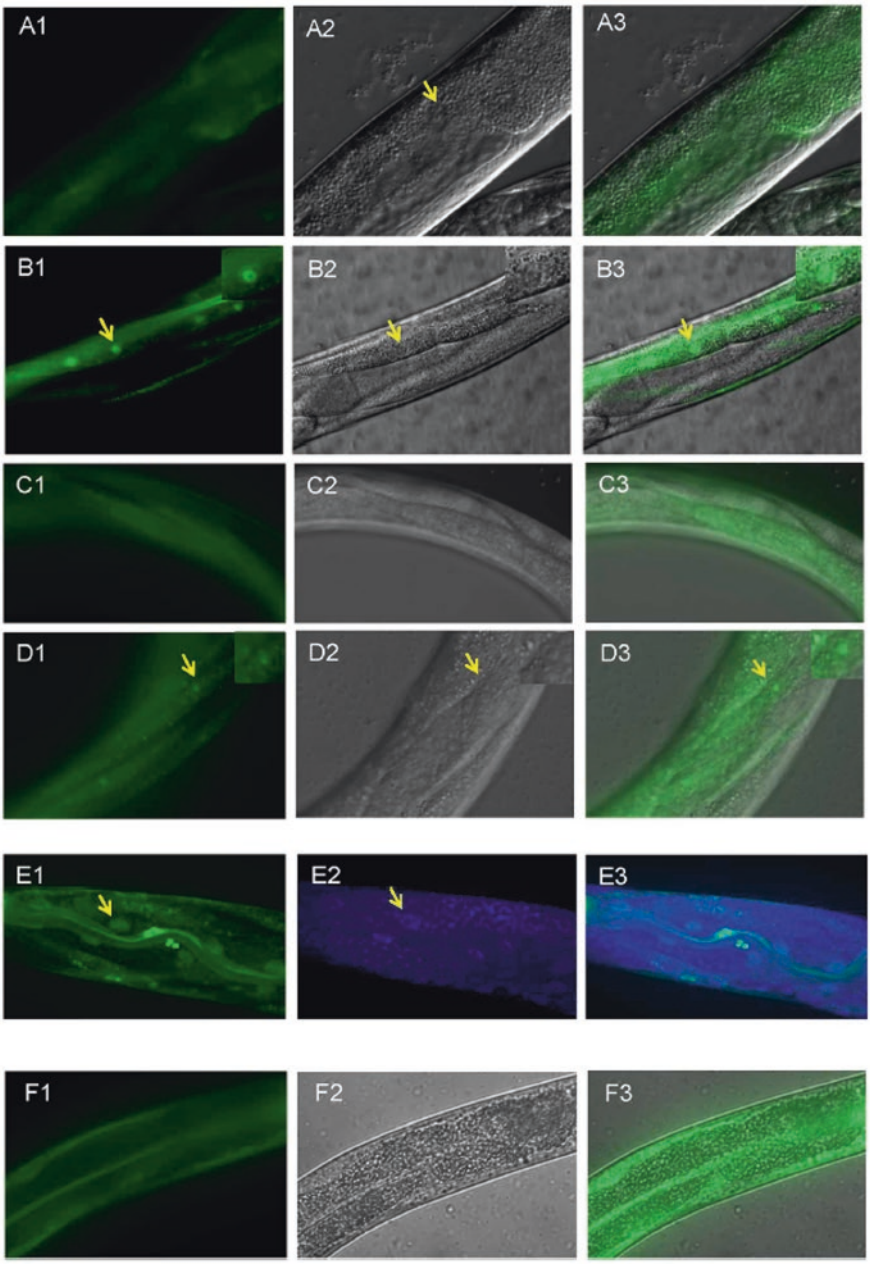

Fig. 10.18 EXL-1 accumulates into the nucleus after heat shock [37]. (A1-A3) EXL-1::GFP is expressed in intestinal cells at standard culture condition (20 °C). The protein is diffuse inside the cells. No exclusion of nuclear expression was observed. (B1–B3) EXL-1::GFP accumulates into the intestinal nuclei (arrows) when animals were subjected to heat shock at 35 °C for 2 h. Inset shows enlarged image of the nucleus. (C1–C3) EXL-1::GFP is expressed in body wall muscle cells.

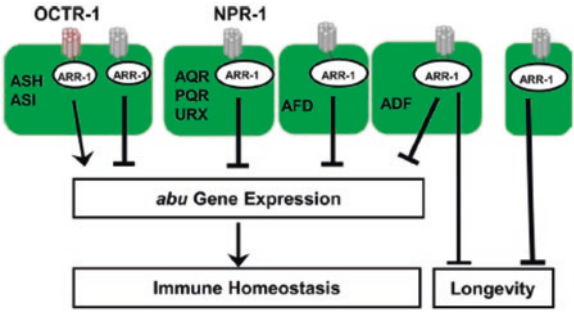

Fig. 10.19 Schematic of neural control of immune homeostasis by ARR-1 signaling [38]. In addition to OCTR-1, at least another receptor may signal through ARR-1 in ASH and ASI neurons to control *abu* gene expression. ARR-1 function in AQR, PQR, and URX neurons appears to play only a small role in the control of *abu* genes, whereas ARR-1 function in ADF and AFD neurons plays a more important role. ARR-1 signaling in ADF neurons also partially regulates longevity. Chemosensory ADF and thermosensory AFD neurons have unidentified receptors that may be regulated by ARR-1 to control *abu* gene expression and immune homeostasis

10.5 G-Proteins

10.5.1 Gqα Signaling

In organisms, Gqα signaling antagonizes Goα signaling by affecting the levels of diacylglycerol (DAG). In nematodes, the Gqα signaling is mediated by heterotrimeric G-protein α q subunit (EGL-30), and EGL-30 stimulates the phospholipase C β (EGL-8) to produce the DAG [39]. Both the *egl-30* and the *egl-8* mutant nematodes have decreased DAG and decreased neuronal secretion [39]. It was further observed that, besides the constitutive DAF-16 nuclear localization, the elevated expressions of antimicrobial genes (*lys-7*, *thn-2*, and *spp-1*) were observed in *egl-8(n488)*, *egl-30(n686)*, and *egl-8(md1971)* mutant nematodes (Fig. 10.20) [40], suggesting the involvement of Gqα and PLCβ in the regulation of innate immune response to pathogen infection. The Gqα and PLCβ mutant nematodes were susceptible to pathogen infection (Fig. 10.20) [40]. Moreover, EGL-30 and EGL-8 were required in the intestine for innate immune response to pathogen infection, but not for longevity [40].

10.5.2 Goα Signaling

GOA-1 is a neuronal G-protein Goα subunit, and EAT-16 is a regulator of G-protein signaling (RGS) protein, functioning downstream of GOA-1. Under the normal conditions, GOA-1 is involved in the control of locomotion, egg-laying, feeding, and olfactory adaptation. In nematodes, exposure to the pore-forming toxins

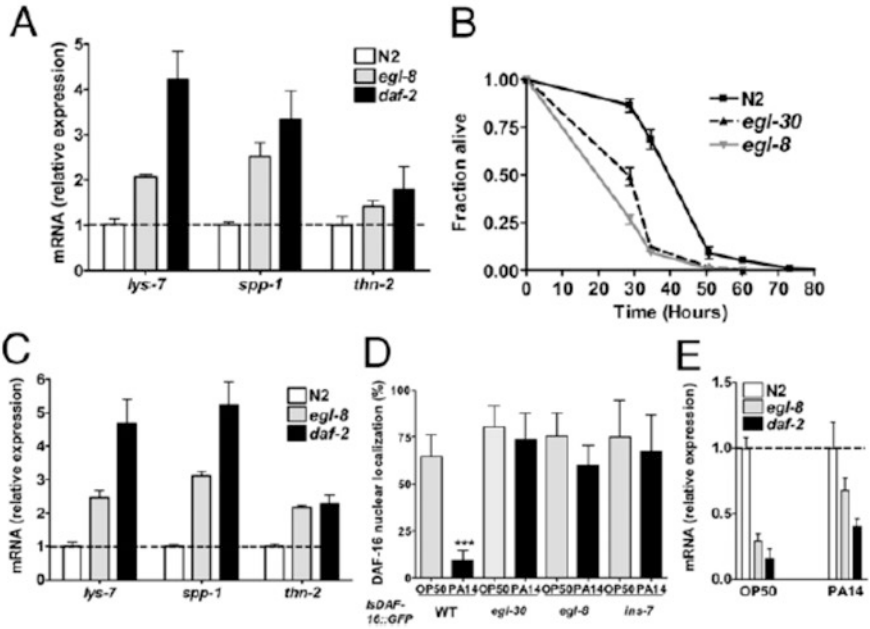

Fig. 10.20 Gqα and PLCβ mutants are sensitive to pathogen despite reduced IIS [40]. (**a**) Elevated expression of IIS-regulated immune genes in *egl-8* mutants. mRNA levels of immune genes in *egl-8(n488)* and wild-type (N2) under conditions of normal growth on *E. coli* as measured by qRT-PCR are shown. (B) Gqα and PLCβ mutants are sensitive to pathogen. Fraction of *egl-30 (n686)*, *egl-8(n488)*, and wild-type (N2) alive are plotted as a function of time of exposure to *P. aeruginosa*. Shown is a representative of three experiments with 100–120 age-matched adults for each strain, mean time to death of 128.5 ± 4.8, 83.7 ± 2.5, and 77.6 ± 2.7 h for N2, *egl-8(n488)*, and *egl-30(n686)*, respectively. Log rank $P < 0.001$ relative to N2. (C–E) *egl-8* mutants maintain reduced IIS upon infection. mRNA levels of *lys-7*, *spp-1*, and *thn-2* (C) and *ins-7* (E) in *egl-8(n488)* and wild-type (N2) after 12 h exposure to *P. aeruginosa* as measured by qRT-PCR. In A, C, and E, mRNA level of each gene was compared with N2, which was set at 1. Shown is the mean ± SD for a representative of three independent experiments. All datasets were significantly different from wild-type ($P < 0.05$; ANOVA Dunnett's test). *egl-8* was not significantly different from *daf-2* in A, B, and E ($P > 0.05$, Dunnett's test). (D) DAF-16::GFP localization in wild-type, *egl-8(n488)*, *egl-30(n686)*, and *ins-7(tm1907)* after exposure to *P. aeruginosa*. The number of nuclei showing distinct DAF-16 localization was enumerated under control (OP50) and infection (PA14) condition. Graph shows a representative of two independent experiments with 20 worms per strain after 21 h of exposure to *P. aeruginosa*. $^*P < 0.001$ (Student's t-test)

(PFTs) induced a feeding cessation [41]. Moreover, it was found that the inhibition of feeding by PFT required both the GOA-1 and the EAT-16 (Fig. 10.21) [41]. Besides this, this Goα signaling was also involved in the regulation of PFT defense in nematodes [41].

In nematodes, the serotonin synthesized in the chemosensory neurons play an important function in modulating the innate immune response [42]. Moreover, it was observed that the Gαo RGS EGL-10 in the rectal epithelium acted downstream of TPH-1-mediated neuronal serotonin signaling released from chemosensory neu-

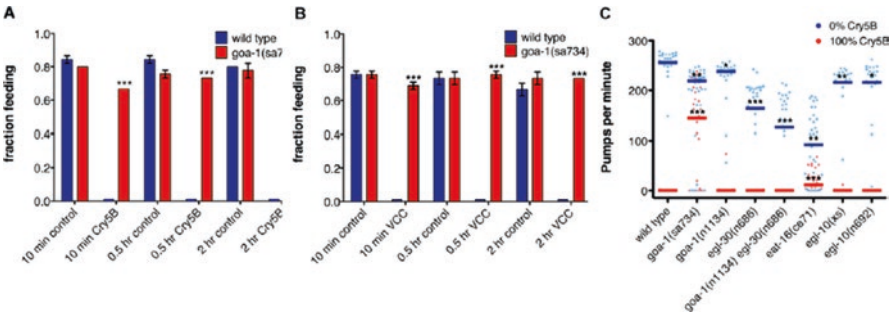

Fig. 10.21 Goα pathway components are required for cessation of feeding in response to PFTs [41]. (**a**) *goa-1(sa734)* mutant animals constitutively feed on *E. coli*-expressed Cry5B. (**b**) *goa-1(sa734)* animals constitutively feed on *V. cholerae* expressing VCC. (**c**) 30 min after transfer to *E. coli*-Cry5B, *goa-1(sa734)* and, to a lesser extent, *eat-16(ce71)* mutant animals have significantly increased feeding rates. Individual measurements of three combined experiments are shown; bars indicate medians

rons to regulate the innate immune response and to affect the pathogen clearance [42]. Different from this, the TPH-1-mediated serotonin signaling might act upstream of, or in parallel to, the EGL-30(Gαq) pathway to regulate the innate immune response [42]. A corresponding hypothesis was further raised about this in Fig. 10.22 [42].

10.6 PLC-DAG-PKD Signaling

10.6.1 PLC-PKD-TFEB Signaling Cascade

The transcription factor EB (TFEB) HLH-30 was required for the host defense [43]. It was further found that the activation of HLH-30 required the DKF-1, a homolog of protein kinase D (PKD) in nematodes infected with *Staphylococcus aureus* [43]. The pharmacological activation of PKD was sufficient to activate the HLH-30 [43], which further confirmed this observation. Moreover, the activation of HLH-30 also required the PLC-1, a phospholipase C (PLC), downstream of Gαq homolog EGL-30 and upstream of DKF-1 in nematodes infected with *S. aureus* [43]. Therefore, a conserved PLC-PKD-TFEB signaling cascade was identified to be required for the regulation of innate immune response to pathogen infection in nematodes (Fig. 10.23) [43].

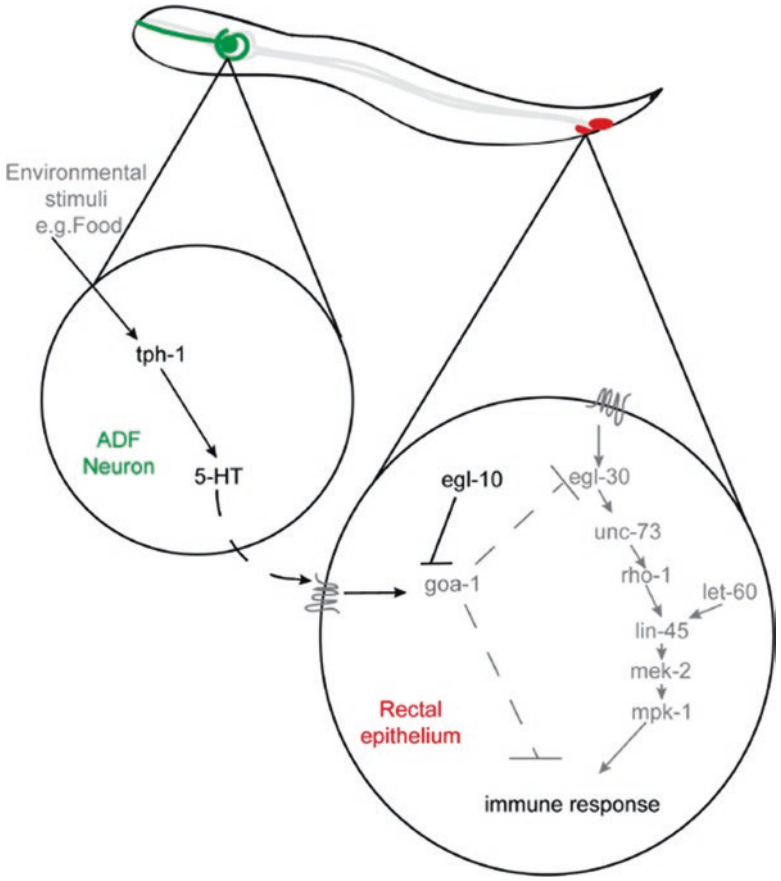

Fig. 10.22 Serotonin synthesis in chemosensory neurons inhibits the immune response by altering rectal epithelial G-protein signaling [42]. In response to environmental cues, such as the presence or absence of food, serotonin, released from ADF chemosensory neurons, acts, directly or indirectly, to regulate GOA-1(Gαo) signaling in the rectal epithelium. This signaling suppresses the Dar phenotype that forms part of the innate immune response and limits the rate of pathogen clearance from the rectal opening

10.6.2 DKF-2

DKF-2 is a protein kinase D (PKD). In organisms, the PKD can mediate the signal transduction downstream from phospholipase C and DAG. In nematodes, pathogen infection could potentially activate the DKF-2 expression [44]. Nematodes lacking DKF-2 were hypersensitive to killing by bacteria [44], suggesting that the DKF-2 regulates the innate immunity. Moreover, TPA-1, a PKCδ homolog, was identified to regulate the activation and the functions of DKF-2 in regulating the innate immunity [44]. Therefore, a signaling cascade of DAG-TPA-1-DKF-2 was raised to be required for the control of innate immunity in nematodes (Fig. 10.24) [44].

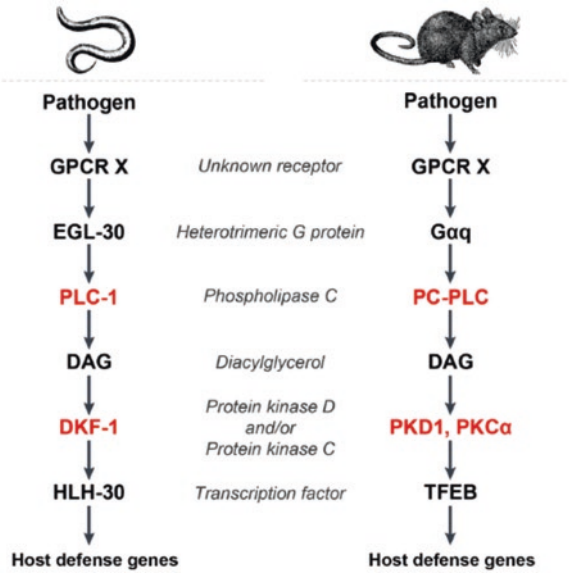

Fig. 10.23 An evolutionarily conserved PLC-PKD-TFEB pathway for host defense [43]

In nematodes, pathogen infection induced the alteration in expression of >75 mRNAs in *dkf-2* mutant nematodes [44]. The products for these altered genes contained those of antimicrobial peptides and proteins that sustain intestinal epithelium [44]. It was further found that the DKF-2 could promote the activation of PMK-1, and a-loop phosphorylation was required for DKF-2-mediated induction of antimicrobial genes [44]. Therefore, the induction of immune effectors by DKF-2 may proceed via PMK-1-dependent and PMK-1-independent pathways in nematodes.

10.6.3 Association with p38 MAPK Signaling

In nematodes, it was further found that the intestinal Gqα and PLCβ could regulate the innate immunity by affecting the activity of p38 MAPK signaling pathway [40]. The PLCβ mutant nematodes had reduced levels of p38 MAPK-regulated immune genes (Fig. 10.25) [40]. That is, the regulation of innate immunity by Gqα-PLCβ signaling is primarily through the intestinal p38 MAPK signaling pathway. Moreover, the intestinal p38 MAPK activity was regulated by the diacylglycerol levels, a product of PLCβ (Fig. 10.25) [40], suggesting that Gqα and PLCβ may modulate the intestinal p38 MAPK activity and innate immunity by further affecting the levels of DAG.

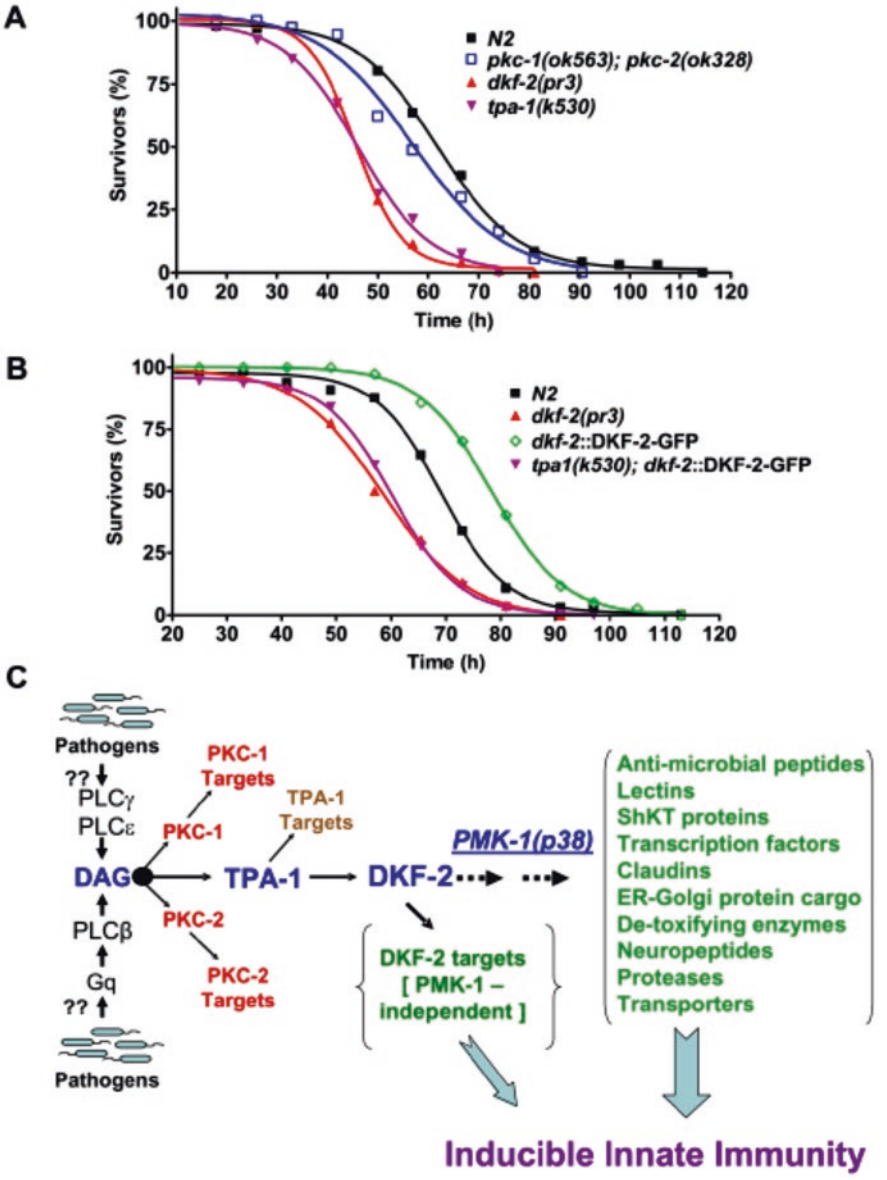

Fig. 10.24 TPA-1 controls DKF-2 [44]. (**a**) Depicts survival curves for *dkf-2(pr3)* null, *pkc-1(ok563);pkc-2(ok328)* double null, and *tpa-1(k530)* defective *C. elegans* mutants feeding on PA14. (**b**) Shows survival curves for WT, *dkf-2(pr3)*, and transgenic (*dkf-2::*DKF-2-GFP and *tpa-1*(k530);*dkf-2::*DKF-2-GFP) nematodes fed PA14. (**c**) Presents a model for (partial) regulation of immunity by a DAG→TPA-1→DKF-2 signaling pathway in *C. elegans*. It is speculated that pathogens directly/indirectly activate PLCs, thereby increasing DAG levels. DAG recruits and activates TPA-1, which phosphorylates and activates DAG-bound DKF-2. DKF-2, a PKD prototype, induces expression of immune effector mRNAs that defend intestinal cells against pathogens via PMK-1-dependent and PMK-1-independent mechanisms

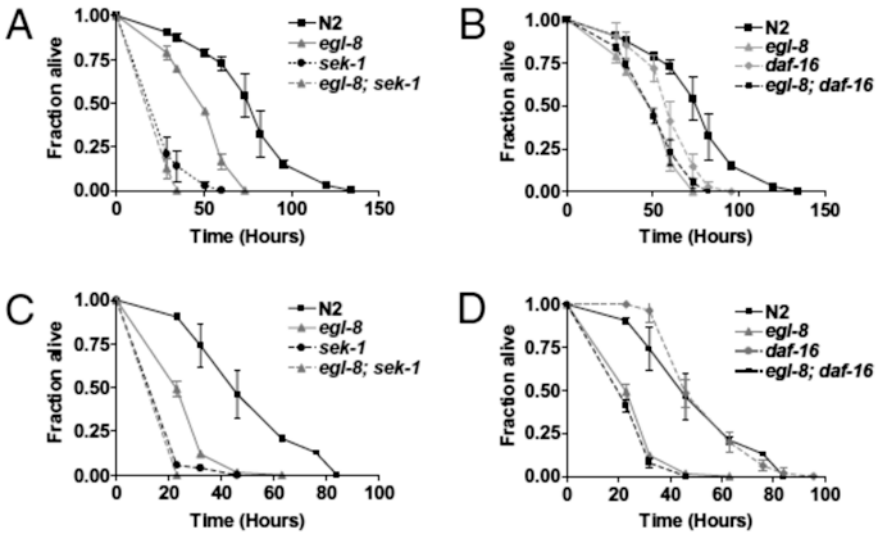

Fig. 10.25 PLCβ influences immunity and oxidative stress resistance primarily through the p38 MAPK pathway [40]. p38 MAPK is the primary mediator of oxidative stress (**a**, **b**) and pathogen (**c**, **d**) sensitivity of *egl-8(n488)*. Graphs show survival of wild-type (N2) and *egl-8(n488)* compared with *sek-1(km4)*, *egl-8(n488); sek-1(km4)* (**a**, **c**) and *daf-16(mu86)* and *egl-8(n488); daf-16(mu86)* (**b**, **d**) after exposure to 3 mM arsenite (**a**, **b**) or *P. aeruginosa* (**c**, **d**). Shown is a representative of two independent experiments for a cohort of 100–120 age-matched adults for each strain

10.7 Ca^{2+} Signaling

10.7.1 UNC-31

UNC-31 is a calcium activator. In nematodes, inhibition of feeding by PFT required the neuronally expressed UNC-31 [41]. The inhibition of feeding by PFT in *unc-31(e928)* mutant nematodes was also different from that in wild-type nematodes, and this maintenance of feeding cessation could be restored when u*nc-31* was selectively expressed in the neurons [41].

10.7.2 CRT-1

crt-1 encodes a calreticulin (CRT), a $Ca2^{+}$-binding protein with the functions in regulating $Ca2^{+}$ homoeostasis and chaperone activity [45]. In nematodes, CRT-1 is expressed in the intestine, pharynx, body wall muscles, head neurons, coelomocytes, and sperm [45]. Besides the reduced mating efficiency, the defects in sperm

development, oocyte development, and/or somatic gonad function in hermaphrodites and the abnormal behavioral rhythms observed in *crt-1* mutant nematodes, the CRT-1 expression was obviously elevated under the stress conditions [45], suggesting the possible involvement of CRT-1 in the regulation of toxicity of environmental toxicants or stresses in nematodes.

10.8 Perspectives

In this chapter, we raised a series of evidence to highlight the crucial roles of GPCRs and ion channels in the toxicity induction of environmental toxicants or stresses. Nevertheless, so far, only very limited GPCRs and ion channels have been identified to be involved in the regulation of toxicity of environmental toxicants or stresses. Actually, there are a huge number of GPCRs existed in the cells of nematodes. However, the exact functions for most of the GPCRs are still unknown even under the normal conditions. Therefore, the systematic elucidation of the functions of GPCRs under both the normal and the stress conditions is needed to be conducted.

At least for nematodes, the responses to environmental toxicants may be very different from those of environmental stresses. The responses of nematodes to environmental toxicants may be closely associated with chemical interaction between toxicants and cells or tissues. However, the response of nematodes to environmental stresses, such as heat shock, UV irradiation, and microgravity, may be more closely associated with the physical interactions. We do not deny that exposure to environmental toxicants and stresses may activate some shared and conserved molecular responses mediated by GPCRs and ion channels. Nevertheless, a certain difference may exist for the molecular responses (mediated by GPCRs and ion channels) to environmental toxicants from those of environmental stresses.

In this chapter, we also tried to introduce and discuss the potential activation of cytoplasmic signaling cascade, especially the signaling cascade containing ARR-1/arrestin, G-proteins, PLC-DAG-PKD signaling, and Ca^{2+} signaling activated in nematodes exposed to environmental toxicants or stresses. Nevertheless, most of the related information about this is still unclear. More detailed and different signaling cascades downstream of the cell membrane GPCRs and ion channels are needed to be further carefully identified, that is, besides the already introduced cytoplasmic signaling cascade here, whether certain GPCRs and especially ion channels will potentially activate or suppress other unknown downstream cytoplasmic signaling cascades. Additionally, it is still unclear how the possible shift will happen between or among different downstream signaling cascades under different conditions in nematodes.

References

1. Wang D-Y (2018) Nanotoxicology in *Caenorhabditis elegans*. Springer, Singapore
2. Ren M-X, Zhao L, Ding X-C, Krasteva N, Rui Q, Wang D-Y (2018) Developmental basis for intestinal barrier against the toxicity of graphene oxide. Part Fibre Toxicol 15:26
3. Xiao G-S, Chen H, Krasteva N, Liu Q-Z, Wang D-Y (2018) Identification of interneurons required for the aversive response of *Caenorhabditis elegans* to graphene oxide. J Nanbiotechnol 16:45
4. Ding X-C, Rui Q, Wang D-Y (2018) Functional disruption in epidermal barrier enhances toxicity and accumulation of graphene oxide. Ecotoxicol Environ Saf 163:456–464
5. Zhao L, Kong J-T, Krasteva N, Wang D-Y (2018) Deficit in epidermal barrier induces toxicity and translocation of PEG modified graphene oxide in nematodes. Toxicol Res 7(6):1061–1070. https://doi.org/10.1039/C8TX00136G
6. Shao H-M, Han Z-Y, Krasteva N, Wang D-Y (2018) Identification of signaling cascade in the insulin signaling pathway in response to nanopolystyrene particles. Nanotoxicology in press
7. Qu M, Xu K-N, Li Y-H, Wong G, Wang D-Y (2018) Using *acs-22* mutant *Caenorhabditis elegans* to detect the toxicity of nanopolystyrene particles. Sci Total Environ 643:119–126
8. Dong S-S, Qu M, Rui Q, Wang D-Y (2018) Combinational effect of titanium dioxide nanoparticles and nanopolystyrene particles at environmentally relevant concentrations on nematodes *Caenorhabditis elegans*. Ecotoxicol Environ Saf 161:444–450
9. Li W-J, Wang D-Y, Wang D-Y (2018) Regulation of the response of *Caenorhabditis elegans* to simulated microgravity by p38 mitogen-activated protein kinase signaling. Sci Rep 8:857
10. Xiao G-S, Zhao L, Huang Q, Yang J-N, Du H-H, Guo D-Q, Xia M-X, Li G-M, Chen Z-X, Wang D-Y (2018) Toxicity evaluation of Wanzhou watershed of Yangtze Three Gorges Reservoir in the flood season in *Caenorhabditis elegans*. Sci Rep 8:6734
11. Xiao G-S, Zhao L, Huang Q, Du H-H, Guo D-Q, Xia M-X, Li G-M, Chen Z-X, Wang D-Y (2018) Biosafety assessment of water samples from Wanzhou watershed of Yangtze Three Gorges Reservoir in the quiet season in *Caenorhabditis elegans*. Sci Rep 8:14102
12. Yin J-C, Liu R, Jian Z-H, Yang D, Pu Y-P, Yin L-H, Wang D-Y (2018) Di (2-ethylhexyl) phthalate-induced reproductive toxicity involved in DNA damage-dependent oocyte apoptosis and oxidative stress in *Caenorhabditis elegans*. Ecotoxicol Environ Saf 163:298–306
13. Xiao G-S, Zhi L-T, Ding X-C, Rui Q, Wang D-Y (2017) Value of *mir-247* in warning graphene oxide toxicity in nematode *Caenorhabditis elegans*. RSC Adv 7:52694–52701
14. Zhao L, Wan H-X, Liu Q-Z, Wang D-Y (2017) Multi-walled carbon nanotubes-induced alterations in microRNA *let-7* and its targets activate a protection mechanism by conferring a developmental timing control. Part Fibre Toxicol 14:27
15. Zhao L, Rui Q, Wang D-Y (2017) Molecular basis for oxidative stress induced by simulated microgravity in nematode *Caenorhabditis elegans*. Sci Total Environ 607–608:1381–1390
16. Wu Q-L, Han X-X, Wang D, Zhao F, Wang D-Y (2017) Coal combustion related fine particulate matter ($PM_{2.5}$) induces toxicity in *Caenorhabditis elegans* by dysregulating microRNA expression. Toxicol Res 6:432–441
17. Ruan Q-L, Qiao Y, Zhao Y-L, Xu Y, Wang M, Duan J-A, Wang D-Y. (2016) Beneficial effects of *Glycyrrhizae radix* extract in preventing oxidative damage and extending the lifespan of *Caenorhabditis elegans*. J Ethnopharmacol 177: 101–110
18. Zhi L-T, Yu Y-L, Li X-Y, Wang D-Y, Wang D-Y (2017) Molecular control of innate immune response to *Pseudomonas aeruginosa* infection by intestinal *let-7* in *Caenorhabditis elegans*. PLoS Pathog 13:e1006152
19. Zhi L-T, Yu Y-L, Jiang Z-X, Wang D-Y (2017) *mir-355* functions as an important link between p38 MAPK signaling and insulin signaling in the regulation of innate immunity. Sci Rep 7:14560
20. Sun L-M, Liao K, Hong C-C, Wang D-Y (2017) Honokiol induces reactive oxygen species-mediated apoptosis in *Candida albicans* through mitochondrial dysfunction. PLoS ONE 12:e0172228

21. Sun L-M, Liao K, Wang D-Y (2017) Honokiol induces superoxide production by targeting mitochondrial respiratory chain complex I in *Candida albicans*. PLoS ONE 12:e0184003
22. Sun L-M, Zhi L-T, Shakoor S, Liao K, Wang D-Y (2016) microRNAs involved in the control of innate immunity in *Candida* infected *Caenorhabditis elegans*. Sci Rep 6:36036
23. Sun L-M, Liao K, Li Y-P, Zhao L, Liang S, Guo D, Hu J, Wang D-Y (2016) Synergy between PVP-coated silver nanoparticles and azole antifungal against drug-resistant *Candida albicans*. J Nanosci Nanotechnol 16:2325–2335
24. Wu Q-L, Cao X-O, Yan D, Wang D-Y, Aballay A (2015) Genetic screen reveals link between maternal-effect sterile gene *mes-1* and *P. aeruginosa*-induced neurodegeneration in *C. elegans*. J Biol Chem 290:29231–29239
25. Reboul J, Ewbank JJ (2016) GPCR in invertebrate innate immunity. Biochem Pharmacol 114:82–87
26. Zugasti O, Bose N, Squiban B, Belougne J, Kurz CL, Schroeder FC, Pujol N, Ewbank JJ (2014) Activation of a G protein–coupled receptor by its endogenous ligand triggers the innate immune response of *Caenorhabditis elegans*. Nat Immunol 15:833–838
27. Powell JR, Kim DH, Ausubel FM (2009) The G protein-coupled receptor FSHR-1 is required for the *Caenorhabditis elegans* innate immune response. Proc Natl Acad Sci U S A 106:2782–2787
28. Styer KL, Singh V, Macosko E, Steele SE, Bargmann CI, Aballay A (2008) Innate immunity in *Caenorhabditis elegans* is regulated by neurons expressing NPR-1/GPCR. Science 322:460–464
29. Yu Y-L, Zhi L-T, Guan X-M, Wang D-Y, Wang D-Y (2016) FLP-4 neuropeptide and its receptor in a neuronal circuit regulate preference choice through functions of ASH-2 trithorax complex in *Caenorhabditis elegans*. Sci Rep 6:21485
30. Yu Y-L, Zhi L-T, Wu Q-L, Jing L-N, Wang D-Y (2018) NPR-9 regulates innate immune response in *Caenorhabditis elegans* by antagonizing activity of AIB interneurons. Cell Mol Immunol 15:27–37
31. Sieburth D, Ch'ng Q, Dybbs M, Tavazoie M, Kennedy S, Wang D, Dupuy D, Rual JF, Hill DE, Vidal M, Ruvkun G, Kaplan JM (2005) Systematic analysis of genes required for synapse structure and function. Nature 436:510–517
32. Sieburth D, Madison JM, Kaplan JM (2007) PKC-1 regulates secretion of neuropeptides. Nat Neurosci 10:49–57
33. E L, Zhou T, Koh S, Chuang M, Sharma R, Pujol N, Chisholm AD, Eroglu C, Matsunami H, Yan D (2018) An antimicrobial peptide and its neuronal receptor regulate dendrite degeneration in aging and infection. Neuron 97:125–138
34. Cho S, Choi KY, Park C (2004) A new putative cyclic nucleotide-gated channel gene, cng-3, is critical for thermotolerance in *Caenorhabditis elegans*. Biochem Biophys Res Commun 325:525–531
35. Estevez M, Estevez AO, Cowie RH, Gardner KL (2004) The voltage-gated calcium channel UNC-2 is involved in stress-mediated regulation of tryptophan hydroxylase. J Neurochem 88:102–113
36. Cai S, Sesti F (2009) Oxidation of a potassium channel causes progressive sensory function loss during ageing. Nat Neurosci 12:611–617
37. Liang J, Shaulov Y, Savage-Dunn C, Boissinot S, Hoque T (2017) Chloride intracellular channel proteins respond to heat stress in *Caenorhabditis elegans*. PLoS ONE 12:e0184308
38. Singh V, Aballay A (2012) Endoplasmic reticulum stress pathway required for immune homeostasis is neurally controlled by arrestin-1. J Biol Chem 287:33191–33197
39. Lackner MR, Nurrish SJ, Kaplan JM (1999) Facilitation of synaptic transmission by EGL- 30 Gqα and EGL-8 PLCβ: DAG binding to UNC-13 is required to stimulate acetylcholine release. Neuron 24:335–346
40. Kawli T, Wu C, Tan M (2010) Systemic and cell intrinsic roles of Gqα signaling in the regulation of innate immunity, oxidative stress, and longevity in *Caenorhabditis elegans*. Proc Natl Acad Sci U S A 107:13788–13793

41. Los FCO, Ha C, Aroian RV (2013) Neuronal Goα and CAPS regulate behavioral and immune responses to bacterial pore-forming toxins. PLoS ONE 8:e54528
42. Anderson A, Laurenson-Schafer H, Partridge FA, Hodgkin J, McMullan R (2013) Serotonergic chemosensory neurons modify the *C. elegans* immune response by regulating G-protein signaling in epithelial cells. PLoS Pathog 9:e1003787
43. Najibi M, Labed SA, Visvikis O, Irazoqui JE (2016) An evolutionarily conserved PLC-PKD-TFEB pathway for host defense. Cell Rep 15:1728–1742
44. Ren M, Feng H, Fu Y, Land M, Rubin CS (2009) Protein kinase D (DKF-2), a diacylglycerol effector, is an essential regulator of *C. elegans* innate immunity. Immunity 30:521–532
45. Park B, Lee D, Yu J, Jung S, Choi K, Lee J, Lee J, Kim YS, Lee JI, Kwon JY, Lee J, Singson A, Song WK, Eom SH, Park C, Kim DH, Bandyopadhyay J, Ahnn J (2001) Calreticulin, a calcium-binding molecular chaperone, is required for stress response and fertility in *Caenorhabditis elegans*. Mol Biol Cell 12:2835–2845